Development of peptide sequences which are able to bind to the surface of titanium and hydroxyapatite

by

Zuzanna Trzcińska

A thesis submitted to the University of Birmingham for the degree of Master by Research.

School of Metallurgy and Materials
College of Physical Science and Engineering
University of Birmingham
2013

Abstract

Titanium implants are commonly used in the replacement of load bearing joints. Poor and slow initial integration of the titanium with the natural bone tissue is the major cause of long postsurgical healing and short life of an implant. This problem can be overcome by the use of biomimetic coatings made of naturally synthesised materials. Hydroxyapatite is the major mineral component of bone tissue and when applied as an implant coating it has shown improved enhancement of the new bone tissue formation. In addition biomolecules such as peptide aptamers, which have the ability to bind electrostatically to inorganic materials in ambient conditions, are currently being researched.

In this research peptide FITC labelled peptide aptamers sequences made of titanium binding, hydroxyapatite binding motifs and hybrid peptides conjugating both sequences, were synthesized and characterized. They were then coated on Ti6Al4V and hydroxyapatite substrates. Fluorescence Microscopy have proved successful attachment of the molecules on the inorganic surfaces. Peptide release rates from the surface were measured in aqueous solutions at different temperatures and pH values, which mimic the different environments implants can be exposed. It was shown that the peptide stability in tested environment is insufficient to provide a long lasting biomimetic coating.

Dedication

Dedykuję tę pracę mojej babci Kazimierze Trzcińskiej i mojemu dziadkowi Józefowi Myślińskiemu. Dziękuję wam za to, że zawsze jesteście bezgranicznie dumni ze swoich wnuków. Mam nadzieję, że będziecie razem z nami cieszyć się z sukcesów jeszcze przez wiele nadchodzących lat.

Acknowledgements

I would like to thank my supervisor Dr Artemis Stamboulis for the ability of pursuing this fascinating research project and for the help and counselling I was getting from her along the way of my work.
I would also like to thank Dr Anna Peacock, Dr Felicity de Cogan and Dr Paula Mendes for the intellectual help I received from them.

I would also like to acknowledge the technical stuff from the School of Metallurgy and Materials as well as technical stuff and Matt Berwick from the School of Chemistry for helping me to use the equipment needed for this research.

Chcę również podziękować moim kochanym rodzicom Hannie i Romanowi Trzcińskim, którzy wspierali mnie na wszelakie sposoby podczas pracy nad tym projektem. To dzięki nim zawsze dążyłam do spełnienia celu i nigdy się nie poddałam.

Table of Contents

List of Abbreviations

6-mer	Peptide sequence made of six amino acids
8-mer	Peptide sequence made of eight amino acids
12-mer	Peptide sequence made of twelve amino acids
°C	Degree Celsius
λ	Wavelength
A, Ala	Alanine
AA	Amino Acid
Ahx	ε-Aminocaproic acid
atm	atmosphere; pressure unit
Boc	N-(tert-Butoxycarbonyl)
BMP-1	Bone Morphological Protein
BSP	Bone Sialoprotein
CD	Circular Dichroism
D, Asp	Aspartic acid
DCM	Dichloromethane
dH_2O	deionized water
DIPEA	N,N - Diisopropylethylamine
DMF	N,N - Dimethylformamide
E, Glu	Glutamic acid
E8, Glu8	Hydroxyapatite binding sequence made of eight glutamic acids, EEEEEEEE
ECM	Extracellular Matrix
ELISA	Enzyme-linked immunosorbent assay

FITC	Fluorescein isothiocyanate, fluorescence dye
Fmoc	Fluorenylmethyloxycarbonyl, N-terminal protection group
G, Gly	Glycine
g	Gram
H, His	Histidine
h	Hour
HAP	Hydroxyapatite, $Ca_{10}(PO_4)_6(OH)_2$
HBTU	O-Benzotriazole-N,N,N',N'-tetramethyl-uronium-hexafluoro-phosphate
HPLC	High Pressure Liquid Chromatography
K, Lys	Lysine
kN	kiloNewton
L, Leu	Leucine
M, Met	Methionine
MS	Mass Spectrometry
m/z	Mass to charge
min	minute
minTBP-1	6-mer Titanium Binding Peptide, RKLPDA
mmol	millimol
mL	milliliter
MW	molecular weight
µm	micrometer
NaCl	Sodium Chloride
nm	nanometer

NPs	Nanoparticles
OPN	Osteopontin
OtBu	tert-butyl
P, Pro	Proline
Pbf	2,2,4,6,7-Pentamethyldihydrobenzofuran-5-sulfonyl
PBS	Phosphate Buffer Saline
R, Arg	Arginine
rpm	rounds per minute
T, Thr	Threonine
t_{max}	maximum temperature
TBP	Titanium Binding Peptide
TBS	Tris Buffer Saline
TFA	2,2,2-trifluoroethanoic acid; Trifluoroacetic acid
Ti	Titanium
Ti6Al4V	Titanium alloy grade 5, contains 6% Aluminum and 4% Vanadium
TIPS	Triisopropylsilane
TiO_2	Titanium(IV)oxide
Tris	2-Amino-2-hydroxymethyl-propane-1,3-diol
UHP	Ultra-High Purity
UV/Vis	Ultraviolet and Visible light
v/v	Ratio Volume A to Volume B
v/v/v	Ratio, Volume of A to volume B to volume C
W, Trp	Tryptophan
w/l/h	width/length/height

z	charge

List of Illustrations

List of Tables

Chapter 1

1. Introduction and Literature Review

1.1 *Joint Replacement*

Bone exhibits one of the most complex architectures produced by living organisms. It contains 70% of mineral calcium phosphate mostly in the form of hydroxyapatite and 20% of organic materials.[1] The complex structure between the two phases is responsible for giving bone its mechanical properties such as fracture toughness, young modulus and strength. In the cases when these properties fail and defects are created, bone regenerates itself with the help of bone forming cells, such as osteoblasts, osteoclasts and osteocytes.[1] These cells are able to repair small defects of bone tissue but in the case of large defects, for example caused by arthritis or cancer, healing is very hard and sometimes almost impossible. The ability to regenerate also depends on the age and lifestyle of the person. For example when an individual is old, has diabetes or is a smoker the healing is much harder to achieve than in healthy younger people.[2] Instead the joints have to be replaced by a synthetic implant. In the UK the number of the load bearing joint replacement surgeries such as hip replacement and is growing every year. In 2011 there were 173,371 joint replacement surgeries performed in England and Wales, both in NHS and independent clinics, which is 9000 more than in 2009.[3] In the USA the budget for the replacement surgeries was 32 billion US Dollars in 2004 and is expected to be 40 times larger in 2030.[1] Current implants last only between 15 to 20 years and then they have to be replaced.[1] These values show the growing need for the improvement of these implants in the future.

The load bearing joint replacement implants when introduced in the body should have biological and mechanical properties which will decrease the possibility of failing by both rejection of an implant by the body and implant mechanical failure. This is why bone substitutes should be osseoinductive and osseoconductive, the rate of its degradation should not be faster than the rate of formation of new bone which the implant is replacing. It should not be cytotoxic otherwise the osteoblasts will not be able to direct implant-bone integration. Its mechanical properties should be as close as possible to those of the natural tissue so that it will not break under the body weight or cause additional discomfort due to too much stiffness. So far creation of an ideal implant which has exactly the same biological, mechanical and chemical properties as bone, has been impossible to do. Ceramic bone minerals like hydroxyapatite (HAP) are bioresorbable and bioactive by promoting cell adhesion, but they are very brittle. Metals on the other hand have much better fracture toughness and strength but are bioinert and the osseointegration progresses slow. For hips and knees brittleness of ceramic materials such as HAP will lead to breaking of an implant so metals such as titanium are the material of choice.

1.2 *Bone-implant interface*

The most crucial time for the implant survival is the first two years after the replacement surgery. During that time fixation of the implant and its integration in the bone occurs,[1] so understanding the exact mechanism leading toward the osseointegration is important for the longevity of an implant.

The first reaction of a body toward prosthesis is creating a conditioning film by adsorption of proteins on the implant surface and then cells on those proteins. [4, 5] The

adsorption of proteins happens via a combination of hydrogen binding, hydrophilic interactions and electrostatic interactions. The first two cases can lead to a change in protein tertiary structure and ultimately denaturation [6-8] so that the cells will not be able to attach, triggering a negative response. However, if the protein will be adsorbed via electrostatic interactions the conformation will not change and a positive signal for the osseoinductive cells adsorption will be observed.[7, 9, 10]

The next step is filling in the gap between the implant and the bone. It has been observed, that the new bone formation on the implant surface precedes 30% faster than the one coming from the bone.[4] The observed bone growth from the implant toward the bone starts with the attachment of proteins such as Bone Sialoprotein (BSP) and Osteopontin (OPN) and osteoblasts to the implant surface initiate the deposition of the bone materials and from the bone toward the implant where the bone repair process occurs.[4] The new created structure which merges together the tissue and implant BSP and OPN have been found in large quantities,[4] it has been also shown that the expression of these two proteins has been significantly increased in new bone formation regions.[11] This leads to the conclusion that these two proteins contribute the most to the bone-implant integration. Therefore an implant structure that can increase the probability of specific proteins adsorption should be able to speed up the integration and decrease the risk of implant rejection.

1.3 *Titanium as implant material*

The titanium alloy Ti6Al4V is one of the most commonly used alloys for load bearing joint replacement. The mechanical properties as well as its low toxicity bring it on the top of list of the materials used in modern prosthetics. It is light weight, has great fracture

toughness and strength as well as good corrosion resistance and biocompatibility, compared to other metals.[7, 8] The mechanical properties of an implant are due to the metallic core, while the chemical properties such as toxicity and corrosion resistance are dictated by the passivation oxide layer which usually forms when the metal becomes in contact with air or water. The oxide film can be of several nm in thickness and consists of rutile (110) and anatase (101) planes.[9, 10] In aqueous solution some of the oxide layer becomes hydroxylated, due to dissociative adsorption of water, and gain amphoteric character as basic $TiOH_2^+$ and acidic TiO^- sites are formed.[12] Both the oxide and hydroxide can interact with biomolecules via hydrogen bonding, electrostatic and hydrophobic interactions.

The attachment of Extra Cellular Matrix (ECM) biomolecules to the titanium surface is the trigger to start the osseointegration.[7, 9, 10] Proteins such as the Bone Sialoprotein attach themselves on the passivation layer attracting bone forming cells such as osteoblasts to spread on the implant surface and to initiate the new bone formation. If the surface of an implant with localized charge or hydrogen binding sites which are different that the one of ECM proteins, then the biomolecule which came in contact becomes denaturated due to the change in tertiary structure.[6-8] This negative response of protein to the surface significantly slows down the healing process and integration of an implant with the bone, by decreasing the amount of functional biomolecules on the surface of an implant.

Various modifications of the titanium implant have been introduced to improve the biocompatibility and osseointegration. Change in surface roughness was proposed as a metallic implant improvement. In this concept porous surface of implant has possibility of interlocking an implant with the natural bone followed by of bone growth inside of the

irregularities.[4] Unfortunately, the *in vivo* studies showed little bone penetration in these pores [3] Another modification of an implant surface is acid etching where the acid in which the implant is immersed changes the chemistry of the surface of an implant. In these technique metal will develop more hydroxyl groups on its surface which are used by ECM entities such as proteins and cells, as sites for electrostatic binding and the initial stage of osseointegration.[4, 13] Another surface modification is applying coating on the surface by plasma spraying.[13] The material to be deposited is heated up to 15000 K and sprayed molten on the surface. The new layer of coating introduces different chemistry due to a coating with different material such as oxide, which can attract ECM entities to bind. This technique is very energy consuming and the metal sprayed as well as the deposit is subjected to very high temperatures. Both plasma spraying and acid etching require very harsh conditions for the surface modification. The new chemistries are also not very selective towards the proteins and cells which will initiate the osseointegration and can attract unwanted entities such as bacteria. To increase the specificity of the surface of the implant, coating metal with material which resembles or mimics the one in the living organism represents an attractive strategy.

Biomimetics is a study concentrated on designing materials, structures and reactions which mimic those existing in living organisms. Biomimetic materials can be both organic and inorganic, and because they are biomimetically derived from structures of natural tissues, they have greater probability of having positive response of Extracellular matrix entities. There are two different approaches in coating the metallic implant with biomolecules substrates for better integration.[4]

1.4 *Improvement of coatings by applying biomimetic coatings*

For millions of years nature has been utilizing the biomolecules such as proteins and peptides to develop many complex structures of inorganic materials. All this is done in mild aqueous solution conditions of pH close to 7.0, 1 atm pressure and room or biological temperature. For some years now, the understanding on how this process is done and how can it be mimicked in the laboratory have been researched. Understanding of the functions of selected peptides would open a way to create the proteins which could be later used as a tool in medicine and other fields like material science.[14-17]

Introduction of the peptide on the titanium can be done in two different ways depending on what the goal is. If positive cell response is the aim then the attachment of integrin binding sequences or growth factors are preferable.[18] At the moment, most studies are done with the RGD peptide sequence which binds to cell integrins.[19] This motif shows promising results in the study of cell attachment *in vitro* but unfortunately when introduced in the body it detaches itself from the surface of the implant due to weak binding interactions with the implant and results in no improvement of cell binding *in vivo*.[1, 18] Binding was improved by the covalent attachment of the RGD sequence to the surface, however this resulted in inhibition of bone growth.[5] It was proposed that this was due to a lack of specificity of RGD towards osteoblasts in vivo leading to unspecific protein attachment. The second approach involved the introduction of an organic layer on the inorganic implant surface by binding of molecules which are able to bind the hydroxyapatite. These molecules will induce creation of a hydroxyapatite

coating, which will be positively recognized by the osteoblasts and will result in attachment of those cells.

Peptide aptamers are organic molecules which bind selected inorganic structures as well as biological moieties.[13, 20-24] These molecules are made of chains of different amino acids connected together with a peptide bond. The amino acids of the sequence allow for the electrostatic and hydrophobic interactions as well as hydrogen bonding, which contribute to attachment and binding functions.

The sequences of peptides with binding abilities have been successfully found by the use of two methods.[21, 23, 24] Firstly, direct sequencing of native mineral binding proteins and the search for similar sequence domains. Peptides found this way bind to the natural minerals of specific crystalline structures but are limited to those which occur naturally. The second approach is based on combinatorial chemistry libraries such as phage display where viruses such as phages, are designed to express sequences of peptides on their head, then these phages are subjected to binding studies with defined materials. If the expressed peptide has an affinity toward the material, the phage will stay attached on its surface and can later be isolated and analysed to establish the peptide sequence. This method successfully led to finding peptide aptamers which usually are not expressed in the living organisms and bind towards many inorganic materials such as Ag, Pt, Cr_2Co_3, and TiO_2. [23-25]

1.4.1 Titanium binding peptide

Sano and Shiba used phage display to find a 12-mer peptide which specifically binds to titanium. They created a peptide phage library that encodes peptides with diversity ~2.7×10^9 and subjected them for binding studies with titanium particles.[8]. In Sano and

Shiba research, phages which were attached to the surface of the titanium were identified and they found that the sequence RKLPDAPGMHTW (Arg-Lys-Leu-Pro-Asp-Ala-Pro-Gly-Met-His-Tyr-Trp) had the strongest adsorption toward this metal.[26] To predict the nature of the attraction and to test which amino acid is responsible for the interaction with the surface they made phages with alanine substituted for each of the amino acid of the sequence. This substitution showed that only the first six N-terminal residues RKLPDA, later named minTBP-1, take part in the binding and that the R1, P4 and D5 are crucial.[26] It is well known that the peptide aptamers use electrostatic interactions to bind to other substrates.[15, 17, 20, 23, 27-29] It is also known that the titanium interfacial layer in aqueous solution is amphoteric due to the hydroxylation of oxide. [7] Based on these findings Sano and Shiba proposed a binding model where positively charged arginine binds with the TiO^- while the negatively charged aspartic acid binds with the $TiOH_2^+$. This finding is similar to that of Roddick-Lanzilotta *et al*. and the binding of lysine, glutamic and aspartic acids to the titanium surface.[9, 10] The role of proline on the other hand was proposed to be responsible for the right conformation of the bend so the two amino acids can both get into contact with the consecutive hydroxylated surface.[8]

Table 1.1 Examples of peptide sequences able to bind the titanium

Peptide name	Peptide sequence	Reference
STB-1	HKKPSKS	[30]
TiBP-1	RPRENRGRERGL	[31]
R5	SSKKSGSYSGSKGSKRRIL	[20]

The binding between the peptide and the surface can be affected if it is coupled to another molecule. The ability to retain its function when integrated with another species

was tested by grafting minTBP-1 to proteins like ferritin[6, 32], BMP-1[18] as well as with RGD sequences[33]. In all cases, besides the binding with BMP-1, significant adsorption of sequences has been observed. The failure in BMP-1 attachment was explained by expression of too small amounts of minTBP-1 for this this protein which has extremely large molecular weight in comparison with the binding ability of the peptide sequence. This didn't affect the ferritin as more minTB-1s were coupled to it. The ability to be coupled to other molecules shows that the peptide can be used for polypeptides with specifically designed motifs or proteins which will have great impact on bioengineering and especially improvement of implant biocompatibility.

It is often observed that the peptide aptamers bind to more than one inorganic surface, although in some cases the selectiveness towards only one moiety is noticed. Sano *et al*. tested the selectivity of the TBP peptide and found that it binds to the Ti, Ag and Si particles with the preference toward Ti, and it does not bind to Fe, Pt, Sn, Zn Cu, and Cr [25]. The preference is not well understood since all of the tested materials are covered with the passivation film, but it has been proposed that the spacing of the titanium oxide plays a significant role.

1.4.2 Hydroxyapatite binding peptide

Bone is made of collagen fibres and hydroxyapatite ($Ca_{10}(PO_4)_6OH_2$, HAP) attached to them. The collagen is not able to initiate nucleation of the HAP, [34, 35] so other proteins from the ECM such as BSP and OPN control this process.[35] It is well established, that the bone forming proteins possess a large amount of negatively charged residues, such as glutamic acids, aspartic acids and phosphoserines.[36] Based on this, it has been proposed that these acidic motifs are major factors for the

hydroxyapatite crystal formation.[34] The exact process in which these molecules are able the initiate the synthesis is not known but based on the fact that they all have acidic character, it was proposed that the positively charged calcium ions suspended in the Extracellular Matrix will be attracted to them.[11, 34, 37, 38] This will create highly positive sites and cause the negatively charged phosphate ions to neutralize the calcium ions leading to the nucleation of calcium phosphate and further maturation of the crystals to HAP due to the appropriate spatial arrangement of amino acids. [34, 36]

Protein sequencing and analysis has yielded many sequences which have the ability to nucleate the HAP formation. BSP has been observed to exist in the bone-implant interface layer in large quantities,[4] its expression is also increased in the *de novo* bone forming areas.[11] This leads to the conclusion that it is a major component of the new bone formation and of implant early integration. This protein is negatively charged due to repeats of the glutamic acids.

Table 1.2: Examples of peptide sequences able to bind to HAP

Peptide name	**Peptide Sequence**	**Reference**
HABP1	CMLPHHGAC	[17]
DMP1	ESQES QESQSEQDS	[39]
E8	EEEEEEEE	[40]

A highly negative oligoglutamic motif is conserved in mammalian BSP. Quantum calculations, performed by Sahai,[41] of the arrangement of calcium ions, phosphate ions and oligoGlu's carboxylates showed the arrangement similar to that of the (001) face of HAP. The Molecular Dynamic studies on the conformation effect of the peptide on Ca/P formation was further studied by Sahai *et al.*[11] In this research it was shown

that the oligoGlu is able to form an α-helix in solution containing calcium and phosphate ions, this causes the formation of equilateral triangle Calcium and Phosphate arrangement typical for HAP crystals hence the nucleation of HAP. If a random coil is observed, the spatial arrangement is not present an amorphous calcium phosphate is formed.[11] Sahai also reported that the equilateral triangle can be observed when the n, n+4 and n+7 negatively charged amino acids are involved in the calcium ions binding and that this amino acid sequence might form helix which will spatially arrange the crystals of calcium phosphate into HAP form [11].

Peptides with nucleating abilities toward certain materials are also able to bind to them. Sawyer confirmed this property for the oligoglutamic acid sequence. In his research, he conjugated the FITC labelled E7 with the RGD sequence, and bound this structure on HAP.[42] Fluorescence microscopy as well as Enzyme-linked immunosorbent assay (ELISA) confirmed the peptide coating on the surface of the HAP disc proving the binding ability of the OligoGlu sequence on the HAP surface. The research done by Wang *et al*. on conjugation of E8 in the polymer substrate also proves the binding ability of this small motif towards the HAP.[43]

1.5 *Aims and Objectives*

The aim of this project is to create a peptide based coating which will have a potential to link the bioceramic material with the titanium alloy implant. In order to do so sequences are designed to be made of various arrangement of two peptide aptamer motifs: titanium binding peptide (minTBP) and hydroxyapatite nucleating sequence (E8). This two aptamers were previously proven to be able to establish electrostatic interactions with respectively HAP and Ti6Al4V. Also these designed peptide

summarised in the Table 1.3 are synthesized and analysed in terms of purity, uniformity of the coating on the respective stability on the surface in the environments which can occur during the postsurgical wound healing.

Table 1.3 Synthesized peptide sequences with the function of titanium and/or HAP binding. The titanium binding domain is underlined with a blue colour and HAP binding domain is underlined with a red colour.

Peptide	Peptide sequence
minTBP	RKLPDA
FITC labelled minTBP	(FITC)-Ahx-RKLPDA
E8	EEEEEEEE
FITC labelled E8	(FITC)-Ahx-EEEEEEEE
minTBPE8	RKLPDA-Ahx-EEEEEEEE
FITC labelled minTBPE8	(FITC)-Ahx-RKLPDA-Ahx-EEEEEEEE
E8minTBP	EEEEEEEE-Ahx-RKLPDA
FITC labelled E8minTBP	(FITC)-Ahx-EEEEEEEE-Ahx-RKLPDA
minTBPminTBPE8	RKLPDA-Ahx-RKLPDA–Ahx-EEEEEEEE
FITC labelled minTBPminTBPE8	(FITC)-Ahx-RKLPDA-Ahx-RKLPDA–Ahx-EEEEEEEE
minTBPminTBP	RKLPDA-Ahx-RKLPDA
FITC labelled minTBPminTBP	(FITC)-Ahx-RKLPDA-Ahx-RKLPDA

They are then analysed in terms of their composition, coating distribution and release from the inorganic surfaces at different pH values and temperatures relevant to wound healing and implant conditions. The determination of whether the peptide is able to establish binding with the inorganic surface and how fast the peptide is released from the surface is then investigated.

Chapter 2

2. Materials and Methods

2.1 *Materials*

All of the Fmoc protected amino acids, amino acid preloaded Wang resin beads (loading 0.21 - 5.3 mmol) and O-benzotriazole-N,N,N',N'-tetramethyl-uronium-hexafluoro-phosphate (HBTU) used in Solid Peptide Phase Synthesis (SPPS) were purchased from NovaBiochem, UK. All of the amino acids had purity of >98% and were obtained with N-terminal Fluorenylmethyloxycarbonyl (Fmoc) protecting group as well as with side chain protecting groups where appropriate. Amino acids and resin beads which were obtained, were Fmoc-Ala-OH, Fmoc-Ala-Wang (loading 0.33 mmol/g), Fmoc-Arg(Pbf)-OH, Fmoc-Asp(OtBu)-OH, Fmoc-Glu(OtBu)-OH, Fmoc-Glu(OtBu)-Wang (loading 0.32 mmol/g), Fmoc-Gly-OH, Fmoc-Gly-Wang (loading 0.78 mmol/g) , Fmoc-Leu-OH, Fmoc-Lys(Boc)-OH and Fmoc-Pro-OH. The solvents and reagents used for SPPS were: anhydrous dichloromethane (DCM), anhydrous N,N-dimethylformide (DMF), N,N-diisopropylethylamine (DIPEA), fluorescein isothiocyanate (FITC), piperidine, ninhydrin as well as cleavage cocktail components: trifluoroacetic acid (TFA) and triisopropylsilane (TIPS). All of the above were purchased from Sigma-Aldrich, were of HPLC grade and they were of >99% purity. Acetonitrile used for the High Pressure Liquid Chromatography (HPLC) was purchased from Sigma-Aldrich, was CHROMASOLV® gradient grade and was of ≥ 99.9% purity. Anhydrous diethyl ether of HPLC grade used for the precipitation of peptides was purchased from Fisher Scientific, UK. Aldrich® System 45™ vessels with cap and fritted disc were used as the reaction flasks during the Solid Phase Peptide Synthesis (SPPS) and were purchased from

Sigma-Aldrich. The Tris Buffer Saline (TBS) 50 mM, pH 7.6 at 24 ^{o}C and 150 mM NaCl tablets were used for dissolving peptides and were purchased from Sigma-Aldrich. The Phosphate Buffer Saline (PBS) 10x, pH 7.4, 100 mM NaCl tablets used for dissolving peptides was purchased from Sigma-Aldrich and they were then diluted with deionized water to the 1M concentration prior to use. Hydroxyapatite (HAP) was made in house following a well-established synthesis route. [44] The titanium alloy substrate was of grade 5 and was supplied by William Gregor Ltd. The polishing plates MD-Piano 220, MD-Largo and MD-Chem used as well as the 9 µm diamond suspension and the colloidal silica (OP-S) were purchased from Struers Ltd.

2.2 *Peptide Synthesis*

Peptides are synthesised when an amide bond (also known as peptide bond) is formed between an amine group (N-terminal) of one amino acid and a carboxylic acid group (C-terminal) of a second amino acid. A simplified peptide bond formation reaction is shown in Figure 2.1, where **R_1** and **R_2** represent different side chain groups.

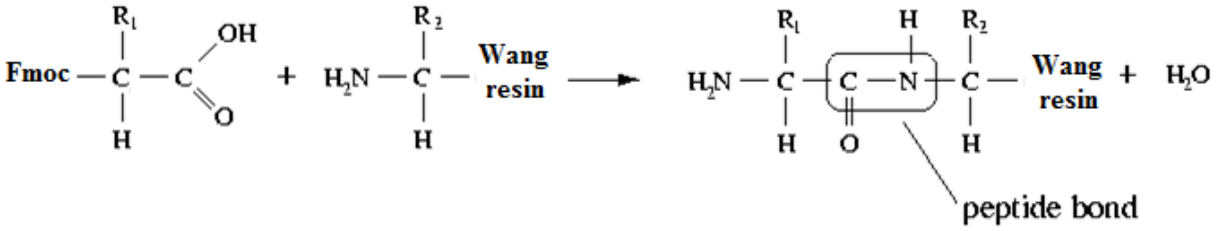

Figure 2.1: Simplified representation of a peptide bond formation between the C-terminal of an amino acid with R_1 side chain and the N-terminal of a second amino acid with R_2 side chain.

Each amino acid is able to react both its N- and C-terminal; this means that the synthesized products of the mixture of amino acids with side chains of **R_1** and **R_2** will be a mixture of dipeptides: R_1R_2, R_2R_1, R_1R_1 and R_2R_2. In addition, when excess of amino

acids are available, longer peptides chains can be formed by joining the di-peptides together. The sequence is controlled by the protection of the C-terminal of the first amino acid and the N-terminal of the second amino acid, as well as capping the side chain reactive groups with appropriate protecting groups.[45] Each protecting group can be cleaved with different reagents. When all of the above conditions are satisfied, peptides of a good purity can be obtained and produced in good yields.

In this research Fluorenylmethyloxycarbonyl (Fmoc) based Solid Peptide Phase Synthesis (SPPS) was performed to ensure purity and yield. In this method, resin beads are linked via ester bonds to the carboxylic acids of an amino acid, while the amine groups are protected with an Fmoc group.[45] The Fmoc is cleaved with base, usually piperidine, while the resin and side chain protecting groups are cleaved with trifluoroacetic acid (TFA).[45] SPPS is a one-pot-synthesis where amino acids are added to the sequence one at a time from the peptides C-terminal towards the N-terminal. The maximum purity of each reaction step is achieved by thorough washing off the excess reagent so they will not react with the consecutive reaction, see Figure 2.2.

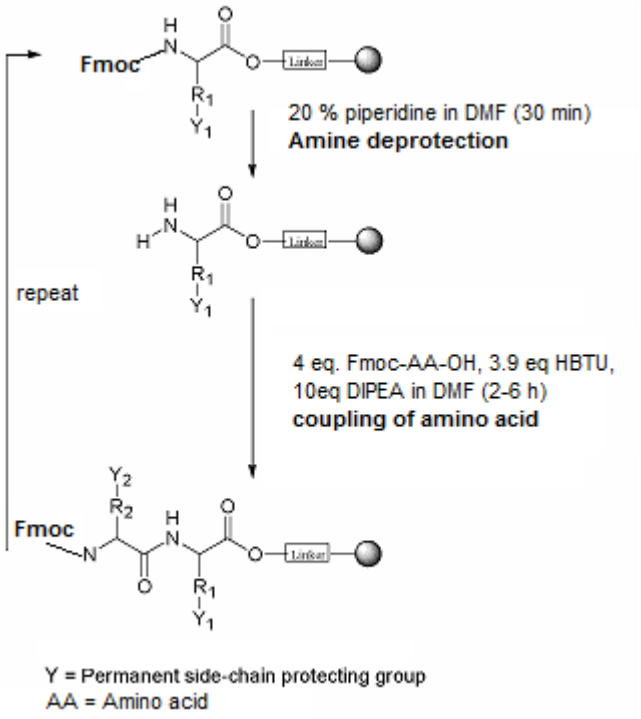

Figure 2.2: Schematic representation of the deprotection and coupling steps performed during Solid Phase Peptide Synthesis. [45]

2.2.1 Deprotection of Fmoc group from N-terminal of amino acid

Cleavage of the Fmoc protection group was performed with the piperidine and the mechanism of reaction is shown in Figure 2.3. Piperidine in DMF (2 mL, 1:5 v: v) was added into the reaction vessel, on the resin beads which were earlier swollen for 1 h in 2-3 mL DMF. The vessel was tightly closed and placed on the orbital shaker. The reaction solution was left to react for 30 minutes under continuous shaking with frequency of 200 rpm. Then the reaction solution was discarded by vacuum filtration and the resin beads, as well as the flask walls were washed three times with DMF (3 mL), three times with DCM (3 mL) and again three times with DMF (3 mL) to ensure that no piperidine is left in the reaction vessel.

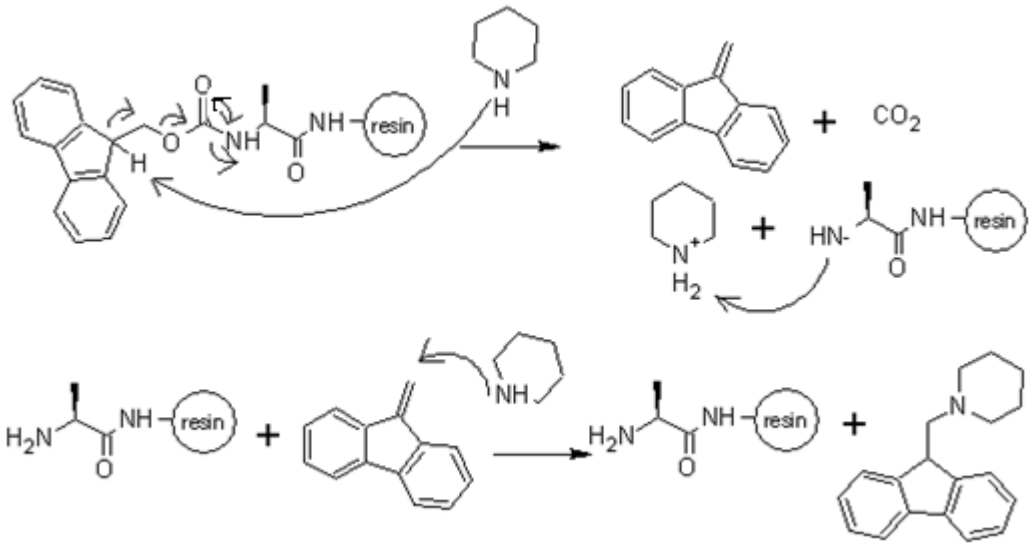

Figure 2.3: Schematic representation of mechanism in deprotection of the Fmoc protection group. [45]

2.2.2 Amide bond formation during Solid Phase Peptide Synthesis

Coupling of the amino acids does not take place spontaneously at ambient temperature so coupling reagents such as O-benzotriazole-N,N,N',N'-tetramethyl-uronium-hexafluoro-phosphate (HBTU) and diisopropylethylamine (DIPEA) are introduced to activate the carboxylic acid by forming reactive intermediates.[46] Schematic mechanism of activation of carboxylic acid by HBTU is shown in Figure 2.4.

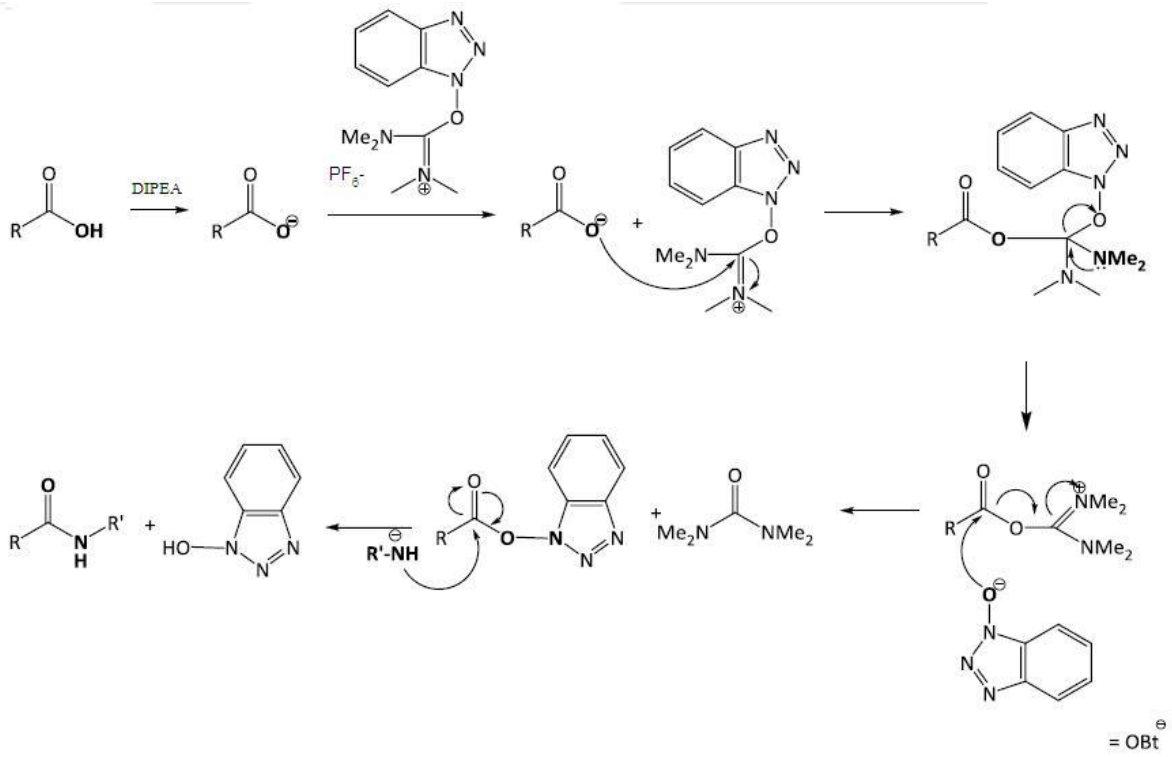

Figure 2.4: Mechanism of peptide bond formation with the use of the HBTU.[45]

The carboxylic acid of the peptide forms an active ester with the HBTU in the presence of DIPEA. The ester bond is later substituted for the amine of an amino acid forming peptide bond.

When the sequence is finished, beads with protected the protected peptide are exposed to a mixture of TFA which will cleave the ester bond between peptide and the resin as well removing the side chain protecting groups. The time of this reaction is crucial to achieve good yield of the product as well as good purity. If the reaction takes place too short the deprotection of the side chain groups will not be finished and the purity will be low.[45]

In this research, the resin beads used were purchased already preloaded with the Fmoc-amino acids and the loading of the resin was between 0.21 - 5.3 mmol. The first step performed was cleavage of the Fmoc group using piperidine followed by washing,

and coupling the deprotected amine group with the second amino acid. Peptide sequences synthesized during SPPS synthesis are summarized in the Table 2.1 all of the peptides were also fluorescence labelled at the end of the synthesis with the fluorescein isothiocyanate (FITC).

Table 2.1: Peptides synthesized by Solid Phases Peptide Synthesis method.

Peptide	**Peptide sequence**
minTBP	RKLPDA
E8	EEEEEEEE
minTBPE8	RKLPDA-Ahx-EEEEEEEE
E8minTBP	EEEEEEEE-Ahx-RKLPDA
minTBPminTBPE8	RKLPDA-Ahx-RKLPDA–Ahx-EEEEEEEE
minTBPminTBP	RKLPDA-Ahx-RKLPDA

The 6-Aminocaproic acid (Ahx) spacer was added to decrease the impact of the bulky fluorescein isothiocyanate (FITC) on the function of the peptide sequence. During the procedure the amount of the reagents added was based on the molar loading of resin beads and the amounts of the reagent is described as the equivalents (eq.). Fmoc-amino acid (5 eq.) HBTU (4.9 eq.) and DMF (2 mL) were added into a clean test tube, mixed with a vortex mixer and left to react for 5 min. Next, DIPEA (10 eq.) was added into the mixture; the solution was mixed with a vortex mixer and transferred to the vessel with deprotected, washed resin beads. Then resin beads and the amino acid containing solution were left to react with shaking (2 h – 3.5 h). Ninhydrin test was used to determine if peptide couplings were complete and it was performed after 2 h of coupling reaction. The test was performed by transferring a small amount of resin (~10 beads)

into a test tube with the solution of ninhydrin in water (2 mL, 1:100 w:v) followed by heating for 3 minutes. No colour change or brown colour of beads after 3 minutes of boiling the solution was an indication of complete coupling, while blue coloured beads was an indication of incomplete coupling. The ninhydrin test was not performed during coupling of leucine with proline because colour change is not observed when secondary the amine of proline is present.

After the coupling reaction was completed the solution in the reaction vessel was discarded and the resin beads as well as the flask walls were washed three times with DMF (3 mL), three times with DCM (3 mL) and again three times with DMF (3 mL). The wash step was followed by deprotection and coupling with the next amino acid as described above till the entire sequence was synthesized.

The resin beads containing complete sequences were dried under vacuum, weighted and one half of the resin was FITC labelled and the rest was cleaved from the resin.

2.2.3 FITC labelling of the peptide sequence

The part of the resin beads designated for fluorescence labelling were swollen in DMF (2 mL, 1 h) and reacted with piperidine in DMF (2 mL; 1:5 v:v) for 30 minutes under shaking conditions on an orbital shaker with the frequency of 200 rpm. Then the solution was discarded and the beads were washed three times with DMF (3 mL), three times with DCM (3 mL) and again three times with DMF (3 mL). Fmoc-Ahx-OH (5 eq.) was added to a test tube and preactivated for 2 minutes in a solution of HBTU (4.9 eq.) dissolved DMF (2 mL) and mixed with a vortex mixer. Then DIPEA (10 eq.) was added and the liquid was mixed again. This solution was then transferred to the resin and reacted with shaking for 1-2 hours depending on results from the ninhydrin test as

described above. When the coupling reaction was completed, the solution was discarded with vacuum filtration and resin beads, as well as the flask walls, washed three times with DMF (3 mL), three times with DCM (3 mL) and again three times with DMF (3 mL). In a test tube fluorescein isothiocyanate (2 eq.) was dissolved in DMF (2 mL) and DIPEA (16 eq.) was added to the solution. This liquid was then transferred to the resin beads and left to react overnight with shaking of 200 rpm frequency. The FITC is prone to photo bleaching so the vessel was shield from the light with aluminium foil during the reaction. Reaction progress was monitored with ninhydrin test as described before. When no primary amines were detected the resin beads were washed four times with DMF (3 mL) and four times with DCM (3 mL) and then dried under vacuum for 15 min.

2.2.4 Cleavage of peptide from the resin and deprotection of amino acid side chains.

The separation of the peptides from the resin beads as well as the deprotection of the side chain protection groups of amino acids were performed with the following steps.

A cleavage mixture of the trifluoroacetic acid (TFA), deionised water and triisopropylsilane (TIPS) (95:2.5:2.5, v: v: v) was prepared fresh for each cleavage reaction. Dried resin beads were placed in a round bottom flask followed by addition of the cleavage solution (10 mL per 0.1 g of dried resin). The flask was closed with a stopper and the solution was left to react with gentle stirring for 3 hours. Flasks with the FITC labelled peptides were additionally wrapped in aluminium foil to prevent the access of light.

2.2.5 Precipitation of peptides

Resin beads were removed by filtration and the filtrate was added dropwise to ice cold diethyl ether resulting in precipitation. The ether solution was then kept overnight at -20 ^{o}C to ensure complete precipitation. The peptide solid was then separated from the supernatant by centrifugation at 13,500 rpm for 3 minutes inside an Eppendorf test tubes and then air dried overnight at -20 ^{o}C. All peptides were stored at -20 ^{o}C.

2.3 *Peptide Characterization*

2.3.1 Mass spectrometry

Peptide sequences were analysed by Electrospray Mass Spectrometry. On a Micromass LCT instrument by the School of Chemistry Mass Spectrometry facility.

2.3.2 High Pressure Liquid Chromatography

The purity of crude peptide products was evaluated using High Pressure Liquid Chromatography (HPLC) on analytical Dionex Summit equipment and was recorded in School of Chemistry. In this technique molecules are separated based on their hydrophobicity by using the octadecyl carbon (C18) chain bonded to the silica as the stationary phase and the mobile phase made of a gradient of solvents, in this case water with 0.05 % TFA 100 % acetonitrile with 0.05% TFA. The eluted molecules were detected by measuring the UV absorbance at $\lambda = 210$ nm, which corresponds to the absorption of the peptide bond. 10 µL of peptide dissolved in water was injected onto an analytical HPLC column and the column was run for 60 minutes with the linear solvent gradient where the 100% of water and 0% of acetonitrile was used at the starting time

and 40% water 60% of acetonitrile was used after 60 min. With the increase of the organic solvent, more hydrophobic molecule were eluted from the column. Purity was based on integration of peaks areas

2.4 *Ti6Al4V and HAP plate preparation and coatings*

2.4.1 Preparation of Ti6Al4V plates

Titanium alloy substrates of 1 cm width, 1 cm length and 0.1 cm thickness were moulded in the conducting Bakelite and polished to a mirror finish on the automatic polishing machine. Three polishing discs were used to polish Ti6Al4V plates. First MD-Piano 220 discs with water as a lubricant was used, than MD-Largo disc with 9 µm diamond suspension followed by MD-Chem disc with ammonia activated colloidal silica with hydrogen peroxide (30%) mixture (OP-S). After polishing, plates were cut out of the conducting Bakelite and were cleaned with ethanol and placed in deionised water overnight. During this time a titanium oxide layer was formed which reacts with water to form hydro-complexes. Prior to coating with the peptides, plates were ultrasonically cleaned in acetone in ultrasonic bath (15 min) followed by rinsing with deionised water followed by ultrasonic cleaning in deionised water (15 min). Samples were then dried in air at room temperature for 1 h.

Titanium alloy substrates were also polished with the carbide paper 400 grit to see if the surface roughness has an effect on the attachment of peptide molecules.

The Ti6Al4V substrates polished to the mirror finish were also treated with the hydrogen peroxide (H_2O_2) to see if the change if this chemical treatment will induce better binding to the surface of the metallic substrates. The each titanium plate was

immersed in 4 mL of 42% hydrogen peroxide and was left to react for 12 h. Afterwards it was rinsed three times with deionised water and it was coated with the peptide immediately.

2.4.2 HAP discs preparation

HAP was prepared from solutions of calcium nitrate tetrahydrite ($Ca(NO_3)•4H_2O$) and ammonium phosphate ($(NH_4)_2HPO_4$), by a well-established method.[47] At first 102 g of $Ca(NO_3)•4H_2O$ was dissolved in 400 mL of deionized water, the pH value was adjusted to 10 with 5 M ammonium hydroxide (NH_4OH) and solution was heated up till 90 ^oC. Then 24 g of $(NH_4)_2HPO_4$ were dissolved in 400 mL of deionized water and pH value of solution was adjusted to 10 with 5 M NH_4OH. Then $(NH_4)_2HPO_4$ solution was titrated into the flask equipped with condenser and containing solution of $Ca(NO_3)•4H_2O$ heated to 90 ^oC. Mixture was left to react for 5 hours at 90 ^oC with constant stirring and reflux. Then solution was placed overnight in the oven at 37 ^oC to achieve mature HAP crystals. The pellet was separated from the supernatant by centrifugation for 10 min at 10000 rpm. The precipitate was then washed three times by resuspending it in deionized water followed by centrifugation for 10 min at 10000 rpm. The obtained HAP was then place in the oven at 60 ^oC until dry. Dried HAP was then grinded with mortar and pestle and compress on the 30 kN load cell into discs (1 cm diameter, 0.7 g) with compression speed of 4 mm/min. The discs were then sintered at 1100 ^oC for two hours with the heating and cooling rate of 4 ^oC per minute. Discs were cleaned before use in ultrasonication bath with ethanol (10 min), and deionized water (10 min) followed by air drying.

Hydroxyapatite (0.5 g) was compressed in a cylindrical dye (1 cm in diameter) with the 5.0 kN maximum load. Then the pellets were placed in the oven, and heated to the sintering temperature of 1100 ^{o}C at a rate of 10 ^{o}C per minute. When this temperature was reached they were sintered for 2 h followed by cooling down to 70 ^{o}C at a cooling rate of 10 ^{o}C per minute.

2.4.3 Measurements of the surface roughness of HAP and Ti6Al4V

The surface roughness of sintered HAP discs and differently treated titanium plates were tested with contact surface roughness analyser (Surtronic 3P, TaylorHobson, UK) set up to measure 99.99 µm range, at 2.5 mm cut off. For analysed substrate six measurements were taken over different points of the surface of a metallic plate. Data were collected in triplicate.

2.4.4 Coating of HAP discs and Ti6Al4V plates surfaces with peptide solutions

Peptides were dissolved in PBS to the final concentration of 100 µg/mL. The plates and discs were placed in 24 well cell culture plates one plate or disc per well. Then a drop (0.5 mL) of peptide solution was dropped on inorganic surfaces and was left to bind for 30 minutes. After this time inorganic surfaces were rinsed three times with deionized water and were air dried.

2.4.5 Fluorescence studies

Surfaces of HAP and Ti6Al4V coated with FITC labelled peptides were analysed under the Nikon fluorescence microscope in the Medical School fluorescence microscopy facility. The Microscope was equipped with a mercury-vapour lamp with UV emission wavelength of 488 nm and a peak emission measured at 525 nm with the FL1 channel. This emission corresponds to the FITC green fluorescence light emission. Three images of each surface were recorded for comparison. ImageJ 1.46r program was used to splitting image into red, blue and green channels. Only the channel green was analysed in terms of grey value as FITC fluorescence is observed as green.

2.5 *Release studies of peptides from the surface of HAP and Ti6Al4V at different temperatures and pH values.*

HAP discs coated with E8, minTBPE8, E8minTBP and minTBPminTBPE8 FITC labelled peptides as well as Ti6Al4V plates coated with minTBP, minTBPE8, E8minTBP, minTBPminTBP and minTBPminTBPE8 labelled peptides were placed one disc per well in the 24 well cell culture plates. Each inorganic material coated with peptides was placed at either 24 ^{o}C, 37 ^{o}C or 44 ^{o}C, pH 7.4 in 2 mL of PBS or at 37 ^{o}C for the temperature dependant release or in 2 mL of sodium acetate buffer pH 5.2, PBS pH 7.4 and phosphate buffer pH 10.0 at a constant temperature of 37 ^{o}C. 50 µL of solution was taken out from each well after 15 min, 30 min, 1 h, 2 h, 3 h, 4 h, 5 h, 6 h, 24 h, 27 h and 30 h. Aliquots were placed in a 96 well cell plate and analysed with a fluorescence microplate reader. The excitation wavelength of 488 nm and FITC light fluorescence

emission was detected at 518 nm. Each release study of peptide was done in triplicate for each temperature and pH value.

By mistake the temperature for the 44 ^{o}C samples was increased to 60 ^{o}C for a period of 15 minutes between the 4 and 5 hour measurement.

The amount of the molecules bounded on the surface was not controlled and can vary from one substrate to another. The impact caused by difference in amount of molecules attached to the substrate was accounted for by dividing each fluorescence intensity data by the highest intensity achieved for a given set. The normalized fractions were then averaged and graphed on a diagram.

Chapter 3

3. Results

3.1 *Solid Phase Peptide Synthesis*

Purity of peptides synthesized during the Solid Phase Peptide Synthesis (SPPS) as well as the theoretical mass and mass observed with the Mass Spectrometry are reported in Table 3.1.

Table 3.1: Purity and Mass Analysis of each synthesized peptide sequence.

Peptide sequence	Peptide sequence	Theoretical mass (g/mol)	Observed mass MS-Spec	Purity
minTBP	RKLPDA	698.8	$[M+H]^{+}$ 699.5 $[M+2H]^{2+}$ 350.2	80%
FITC labelled minTBP	(FITC)-Ahx-RKLPDA	1201.4	$[M+2H]^{2+}$ - 601.2	81%
E8	EEEEEEEE	1050.9	$[M+H]^{+}$ - 1051.2	87%
FITC labelled E8	(FITC)-Ahx-EEEEEEEE	1553.5	$[M+2H]^{2+}$ - 779.4	77 %
minTBPE8	RKLPDA – Ahx-EEEEEEEE	1844.7	$[M+2H]^{2+}$ - 923.3 $[M+3H]^{3+}$ - 615.9	73%
FITC labelled minTBPE8	(FITC)-Ahx-RKLPDA-Ahx-EEEEEEEE	2349.4	$[M+2H]^{2+}$ - 1174.4 $[M+3H]^{3+}$ - 783.3	81%
E8minTBP	EEEEEEEE-Ahx-RKLPDA	1844.7	$[M+2H]^{2+}$ - 923.0 $[M+3H]^{3+}$ - 615.7	80%
FITC labelled E8minTBP	(FITC)-Ahx EEEEEEEE-Ahx-RKLPDA	2349.4	$[M+H]^{+}$ - 1174.5 $[M+2H]^{2+}$ - 783.3	67%
minTBPminTBPE8	RKPLDA-Ahx-RKLPDA-Ahx-EEEEEEEE	2639.4	$[M+2H]^{2+}$ - 1329.1 $[M+3H]^{3+}$ - 886.5	69%
FITC labelled minTBPminTBPE8	(FITC)-Ahx-RKLPDA-Ahx-RKLPDA-Ahx-EEEEEEEE	3145.4	$[M+NH_3]^{+3}$ -1054.0	55%
minTBPminTBP	RKPLDA-Ahx-RKLPDA	1493.6	(M+H) 1329.2 (M+2H) 665.1	77%
FITC labelled minTBPminTBP	(FITC)-Ahx-RKLPDA-Ahx-RKLPDA	1997.3	$[M+2H]^{2+}$ - 998.5 $[M+3H]^{3+}$ - 665.7	64%

3.2 Surface roughness measurements of HAP and Ti6Al4V

Average surface roughness (Ra) of mirror finish polished, carbide paper grit 400 polished and H_2O_2 pre-treated Ti6Al4V plates are summarized in Table 3.2.

Table 3.2: Surface roughness measured for the surfaces of HAP and Ti6Al4V, n = 5.

Surface	Surface roughness (Ra) [µm]
HAP	1.52 ± 0.30 µm
Mirror finish polished Ti6Al4V	0.03 ± 0.01 µm
Carbide paper grit 400 polishing	0.77 ± 0.22 µm
H_2O_2 pre-treatment	1.16 ± 0.16 µm

3.3 Characterizations of the peptide coatings on the surface of the inorganic substrates

FITC labelled peptides coated on the surfaces of HAP and Ti6Al4V were observed under the fluorescence microscopy at the magnification of 10 x (if not specified otherwise) and using 10 ms or 200 ms camera exposure respectively. Longer exposure time was needed for the metallic substrate was needed because, FITC fluorescence was not observed for 10 ms exposure.

Images of FITC labelled peptide coated surface of hydroxyapatite, Ti6Al4V polished to the mirror finish, Ti6Al4V polished with carbide paper and Ti6Al4V treated with the hydrogen peroxide are shown in this section. Grey value intensity distribution across the surface is also included to show how uniform or not uniform the peptide coating is on the surface.

3.3.1 Fluorescence microscopy image of the FITC labelled peptides on the surface of HAP.

Figure 3.1 -Figure 3.5 show fluorescence images as well as the corresponding grey value intensity distribution of E8, E8minTBP, minTBPE8 and minTBPminTBPE8 coated on HAP discs as well as controls prepared with the HAP and PBS buffer. The grey value distribution shows uniform coating with some darker regions which are due to the porous surface of hydroxyapatite.

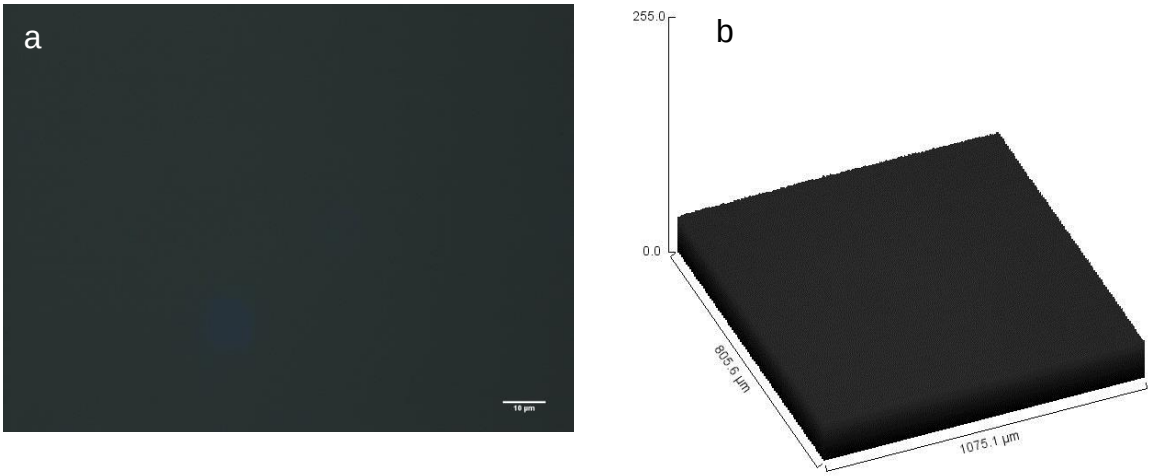

Figure 3.1: a) Fluorescence microscopy image of HAP control and b) gray value distribution of the imaged surface.

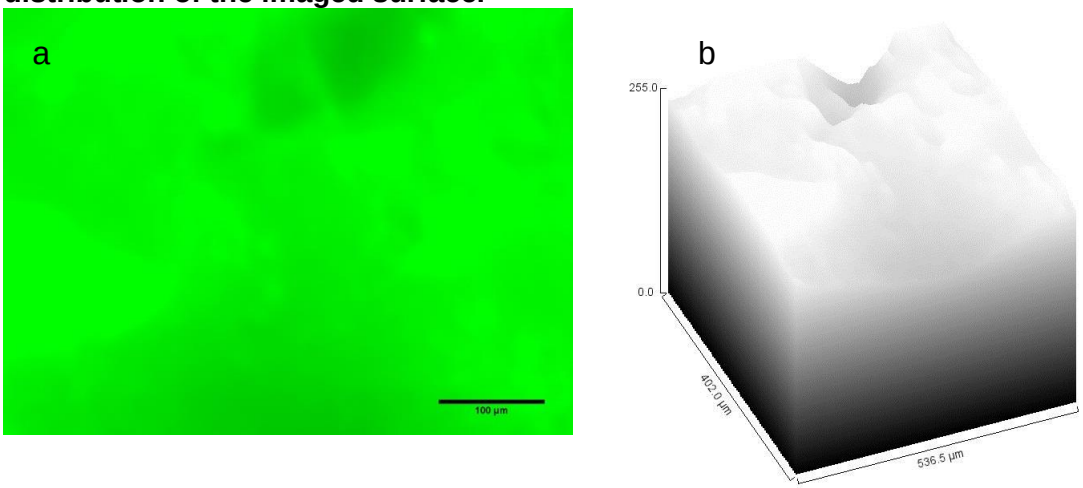

Figure 3.2: a) Fluorescence Microscopy image of HAP coated with the E8 peptide and b) gray value distribution of this molecule across the imaged surface.

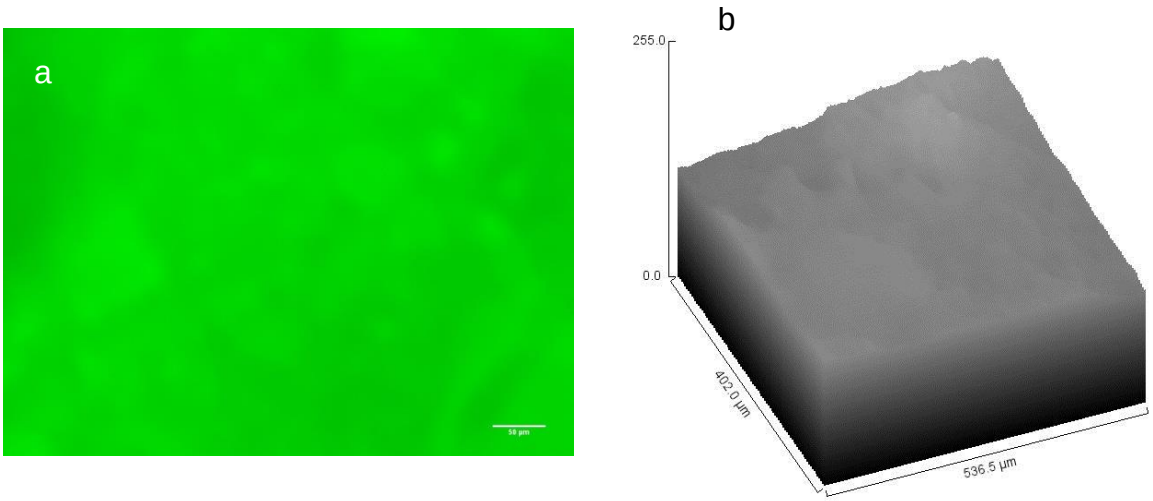

Figure 3.3: a) Fluorescence Microscopy image of HAP coated with the minTBPE8 peptide and b) gray value distribution of this molecule across the imaged surface.

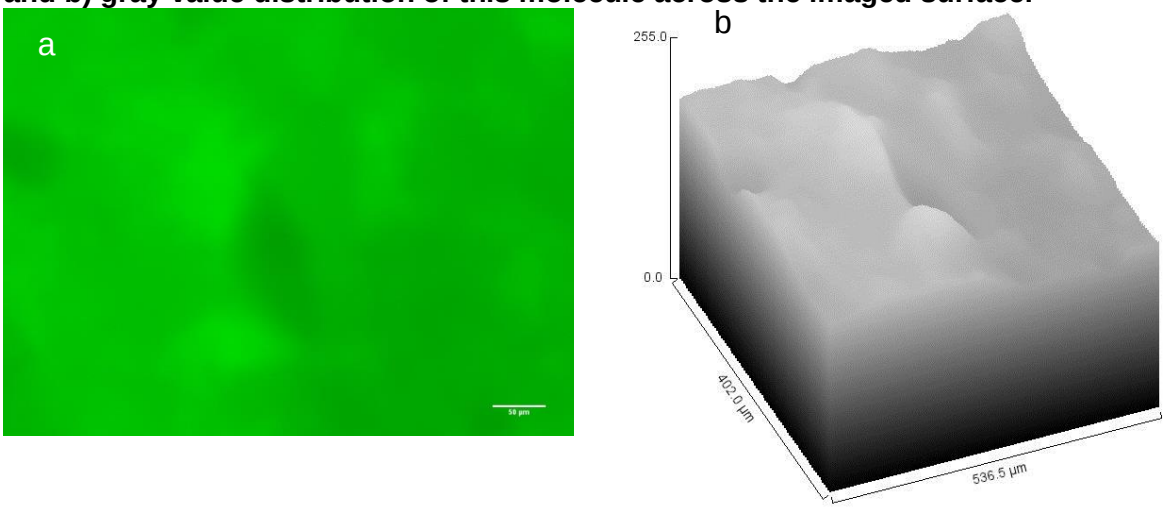

Figure 3.4: a) Fluorescence Microscopy image of HAP coated with the E8minTBP peptide and b) gray value distribution of this molecule across the imaged surface

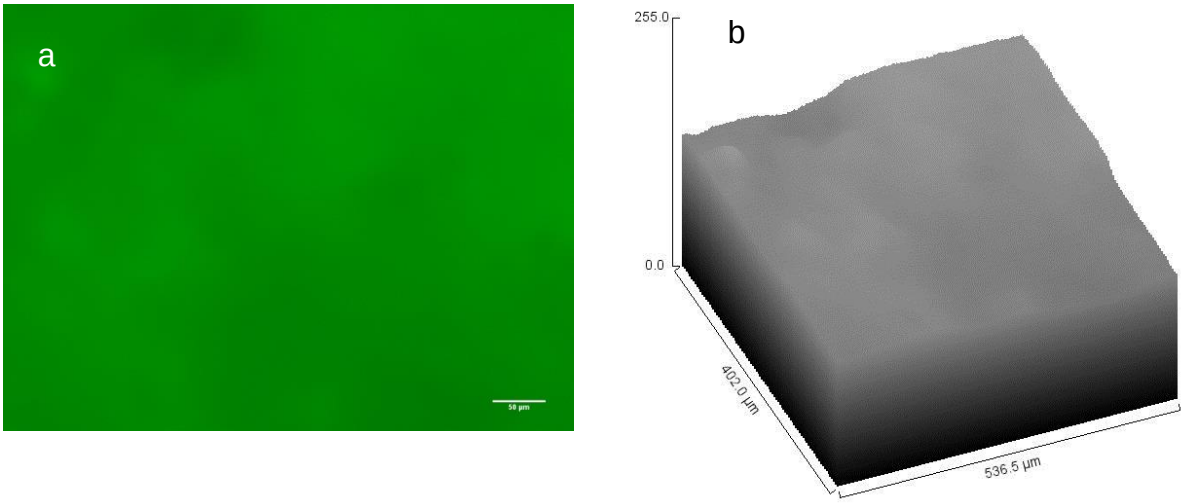

Figure 3.5: a) Fluorescence microscopy image of HAP coated with the minTBPminTBPE8 peptide and b) gray value distribution of this molecule across the imaged surface.

Mean of grey values of imaged surfaces of all the peptides is summarized in Figure 3.6. It was observed that HAP surface coated with the E8 peptide on its own has the greatest intensity out of all the peptides which indicates that this peptide bounded on the surface in the greatest amount. The second greatest intensity was observed for minTBPE8 peptide which has the oligoglutamic acid rich motif at the C terminal of the peptide. E8minTBP which has a third greatest grey value mean intensity has the E8 group between the FITC-Ahx labelling and the minTBP peptide. MinTBPminTBPE8 was observed to have the smallest intensity out of all of the peptides. This peptide has the longest chain and the longest peptide sequence in comparison to the E8 hydroxyapatite binding site.

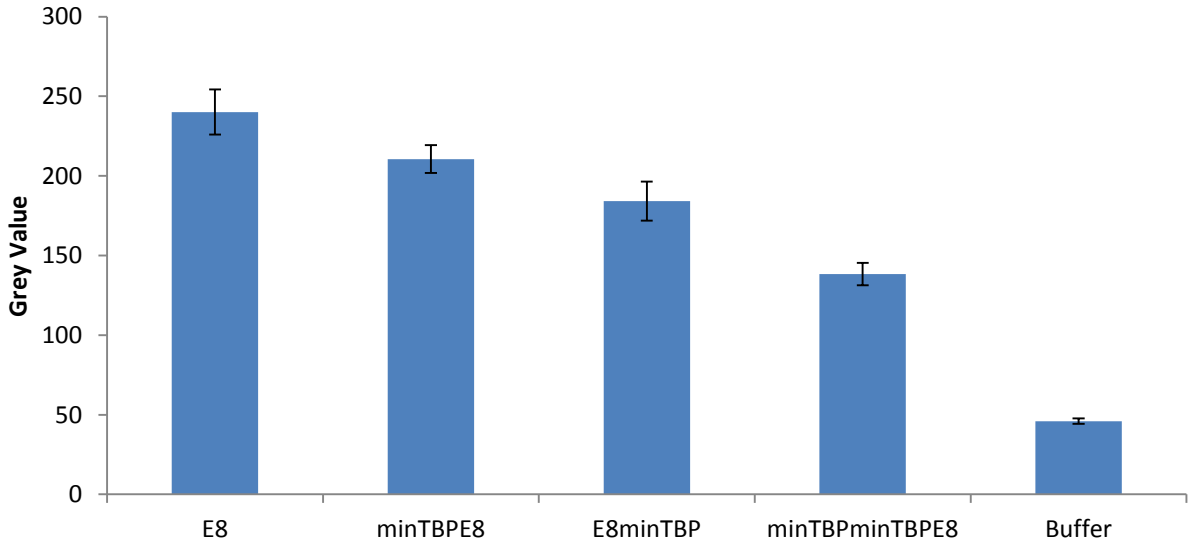

Figure 3.6: Mean grey value intensities of HAP surface coated with peptides. Error bars designate standard deviation for n = 3.

3.3.2 Fluorescence microscopy of the FITC labelled peptides on the surface of mirror finish polished Ti6Al4V

Figure 3.7 Figure 3.12 show fluorescence images as well as the corresponding grey value intensity distributions of minTBP, E8minTBP, minTBPE8, minTBPminTBP and minTBPminTBPE8 coated on mirror finish polished Ti6Al4V plates as well as buffer control. The distribution for all of these molecules was not uniform across the surface. Each of the peptides showed aggregation either in form of crystalline-like arrangements or round shaped clusters.

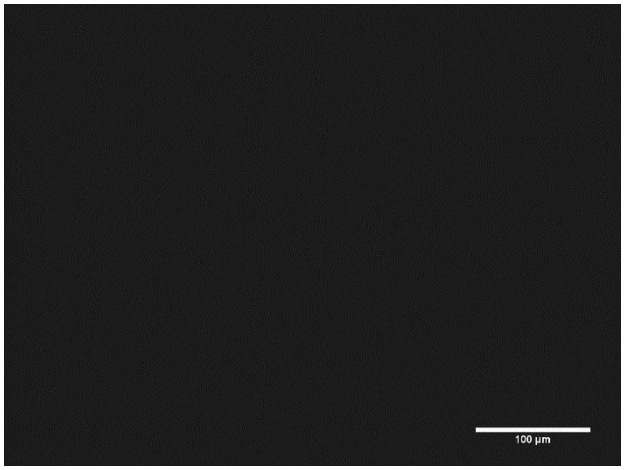

Figure 3.7: Fluorescence microscopy image of the buffer coated control of mirror finished polished Ti6Al4V

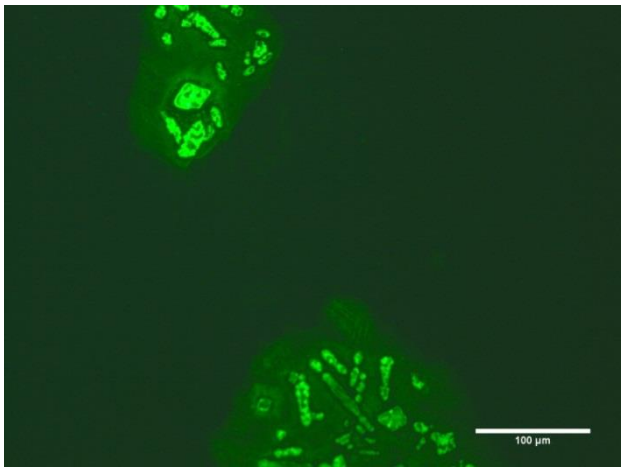

Figure 3.8: Fluorescence microscopy image of mirror finished polished Ti6Al4V coated with the minTBP.

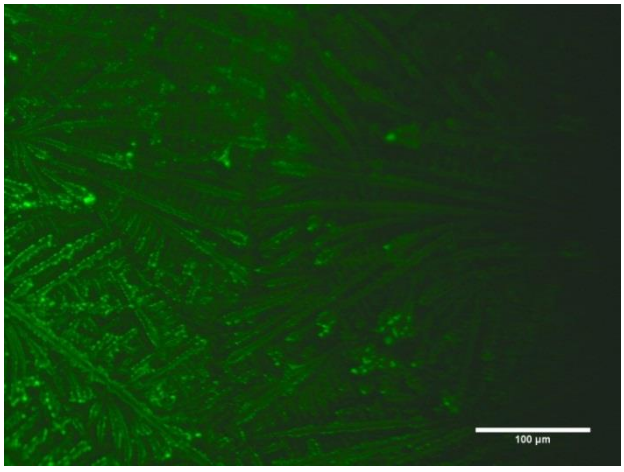

Figure 3.9: Fluorescence microscopy image of mirror finished polished Ti6Al4V coated with minTBPE8 peptide.

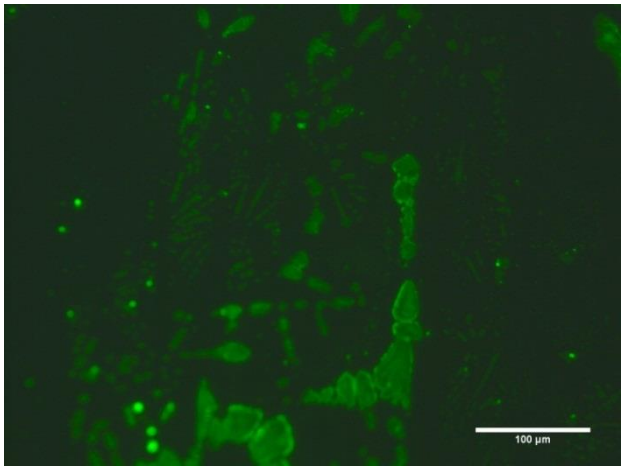

Figure 3.10: Fluorescence microscopy image of mirror finished polished Ti6Al4V coated with E8minTBP peptide.

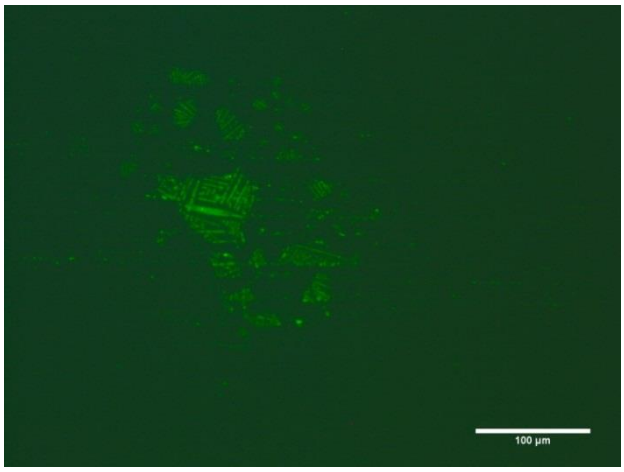

Figure 3.11: Fluorescence microscopy image of mirror finished polished Ti6Al4V coated with minTBPminTBP peptide.

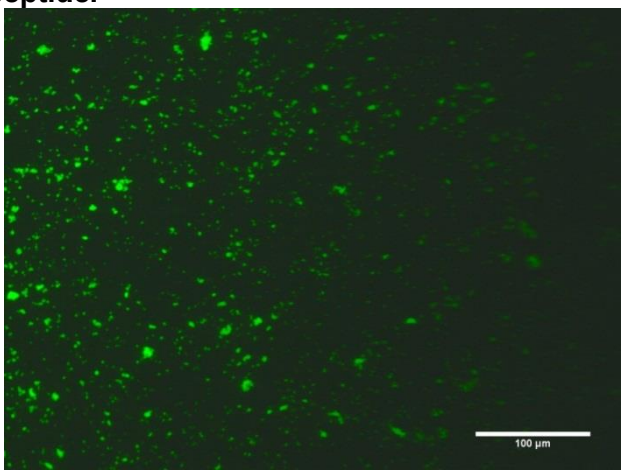

Figure 3.12: Fluorescence microscopy image of mirror finished polished Ti6Al4V coated with minTBPminTBPE8 peptide.

The patterns of the peptide clusters are not similar. MinTBP forms four arm star like shapes, minTBPE8 aggregates in dendroid shapes, E8minTBP was observed as linear and rectangular shapes, minTBPminTBP was observed to form liner shapes and minTBPminTBPE8 was observed as points dots across the titanium surface.

The average of grey values of the surface of Ti6Al4V coated with five studied peptides and a PBS buffer control are shown in Figure 3.13.

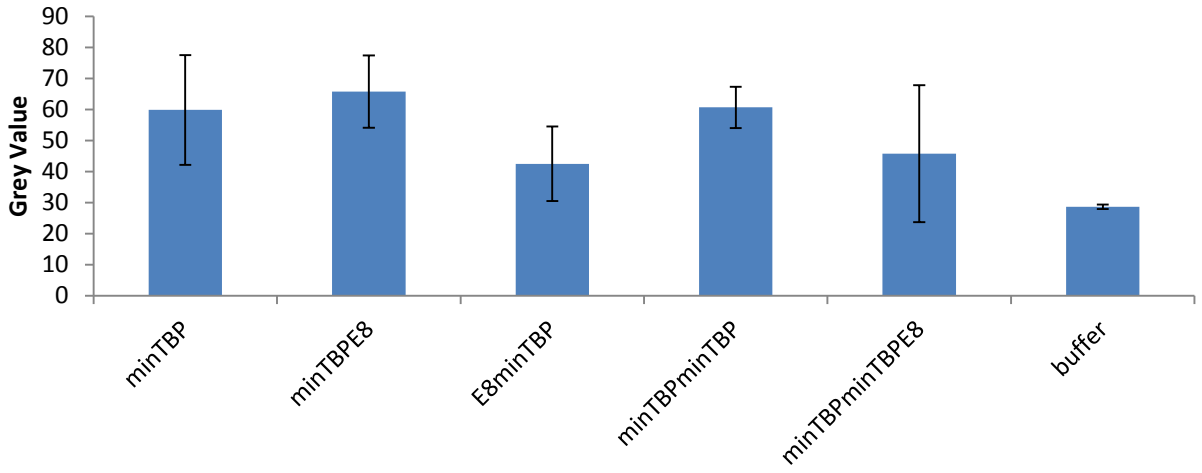

Figure 3.13: Mean grey value intensities of the entire surface of mirror finish polished Ti6Al4V of the five studied peptides and control. Error bars designate standard deviation for n = 3.

Comparison of the grey values of the peptides with both titanium and HAP linker, coated these two surfaces are shown in Figure 3.14. The surface of HAP showed much larger grey value for all of the peptides than the surface of Ti6Al4V.

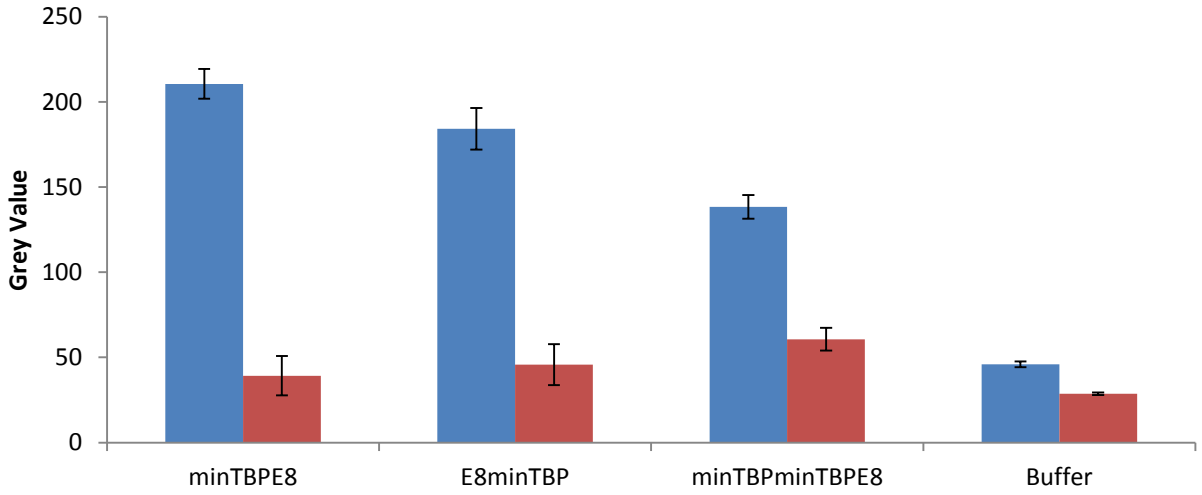

Figure 3.14: Mean grey value intensities of peptides on both HAP and Ti6Al4V surfaces. Error bars designate standard deviation for n = 3.

3.3.3 Fluorescence microscopy imaging of peptides coated on the carbide paper polished and hydrogen peroxide treated Ti6Al4V.

Surfaces of Ti6Al4V polished with the carbide paper as well, or with H_2O_2, were also coated with peptides: minTBP, minTBPE8, E8minTBP, minTBPminTBP, minTBPminTBPE8. Fluorescence imaging shows a uniform coating of the peptides on the surface. On the surfaces of carbide paper polished titanium the distribution of the peptides is uniform with the visible holes which were not removed during polishing. Uniform peptide coverage is also found on the surface of the H_2O_2 treated Ti6Al4V with porous surface topography. The pores were created with the hydrogen peroxide through a process, which is well described in the literature [48]. This unequal surface causes the attached peptides to be at different levels. For the regions where the peptide is attached at the bottom of a pore, FITC intensity is if low as the detection from the camera is less

sensitive than at the higher surface planes where the camera records the intensity as higher.

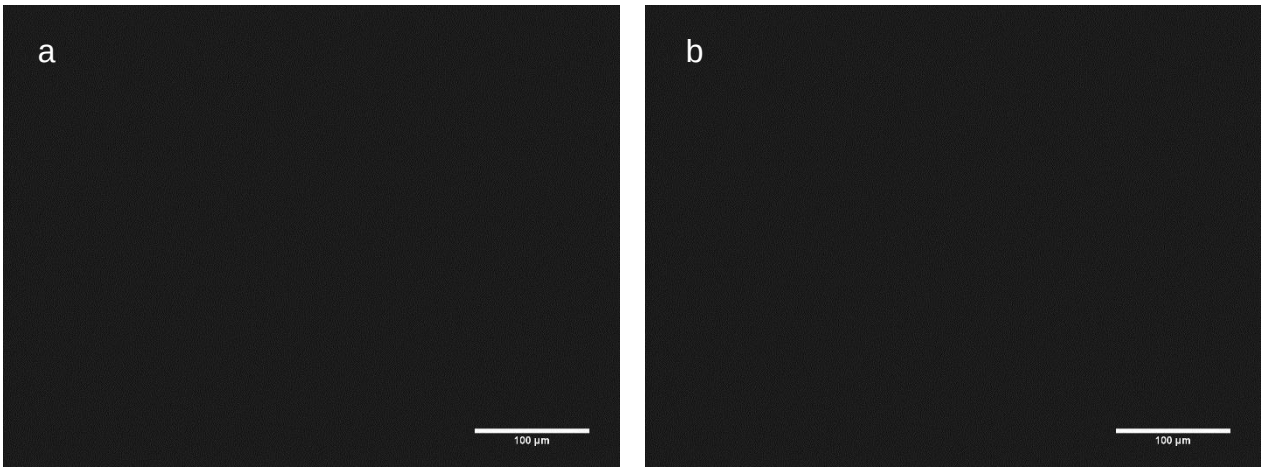

Figure 3.15:Ti6Al4V surface immersed in the PBS buffer control: a) carbide paper polished Ti6Al4V, b) hydrogen peroxide treated.

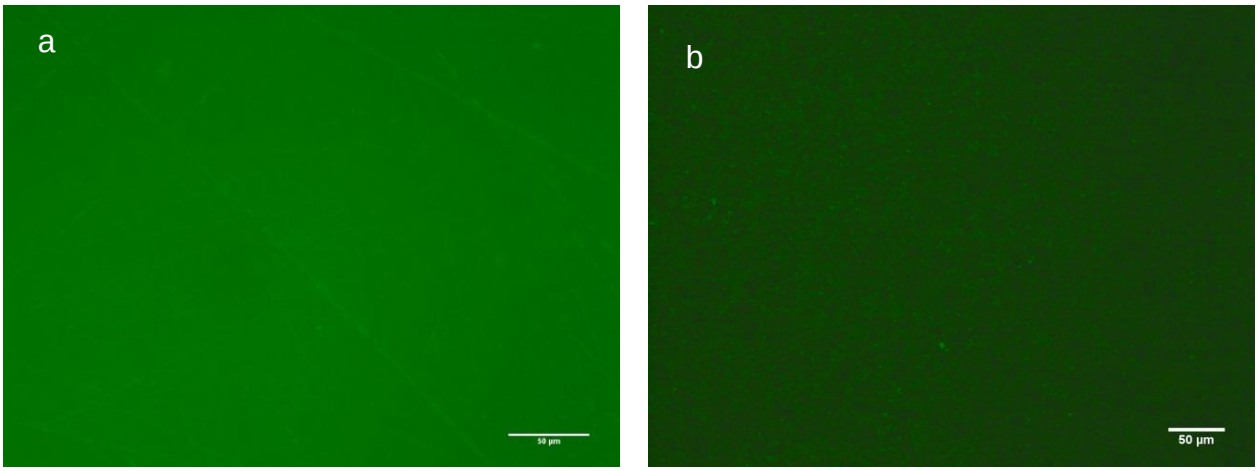

Figure 3.16: Ti6Al4V surface coated with minTBP but with different surface pre-treatment: a) carbide paper polished Ti6Al4V, b) hydrogen peroxide treated.

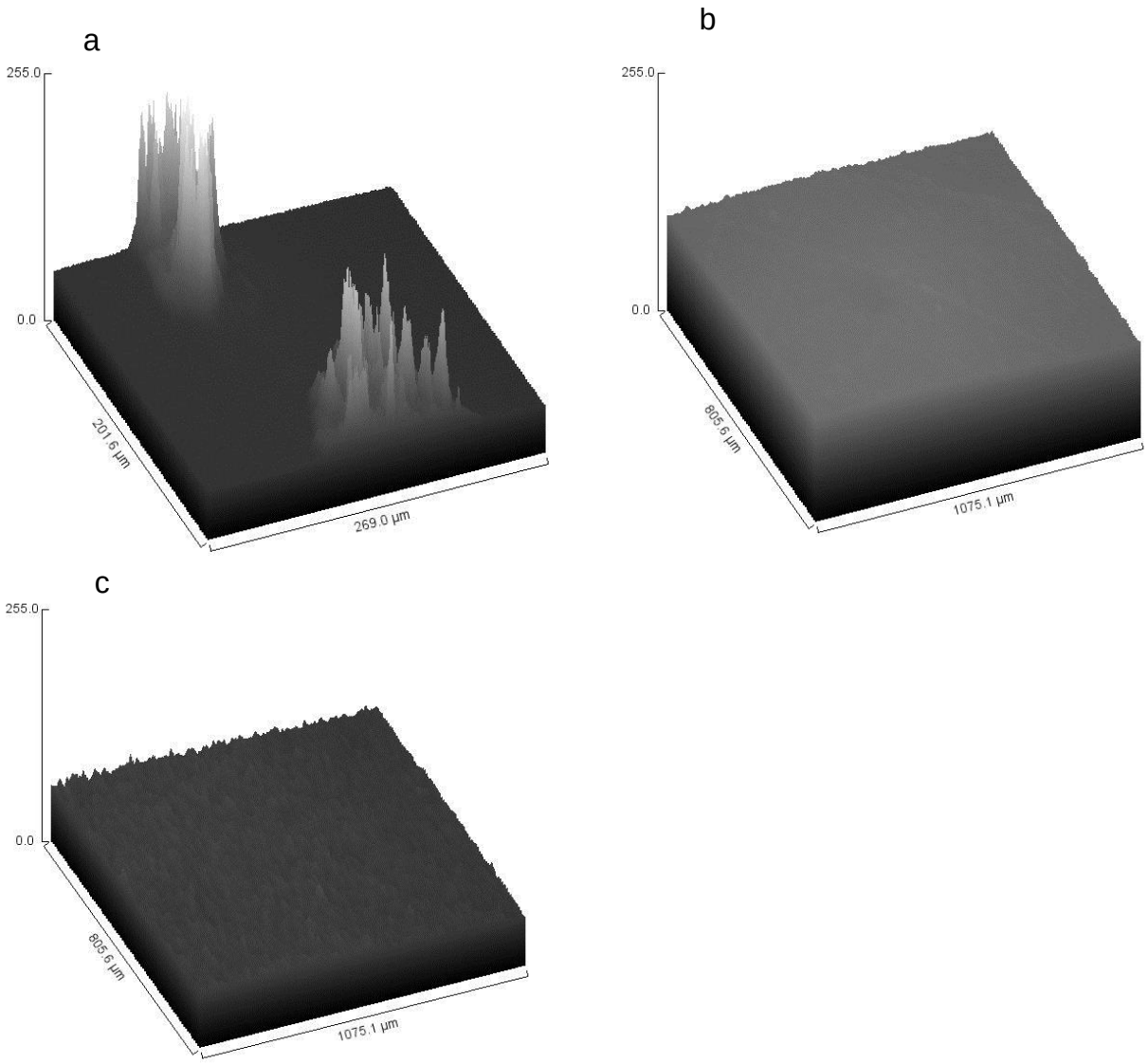

Figure 3.17: Grey value distribution of minTBP peptide coated on the surface of a) mirror finish polished Ti6Al4V, b) carbide paper polished Ti6Al4V and c) hydrogen peroxide pre-treated Ti6Al4V.

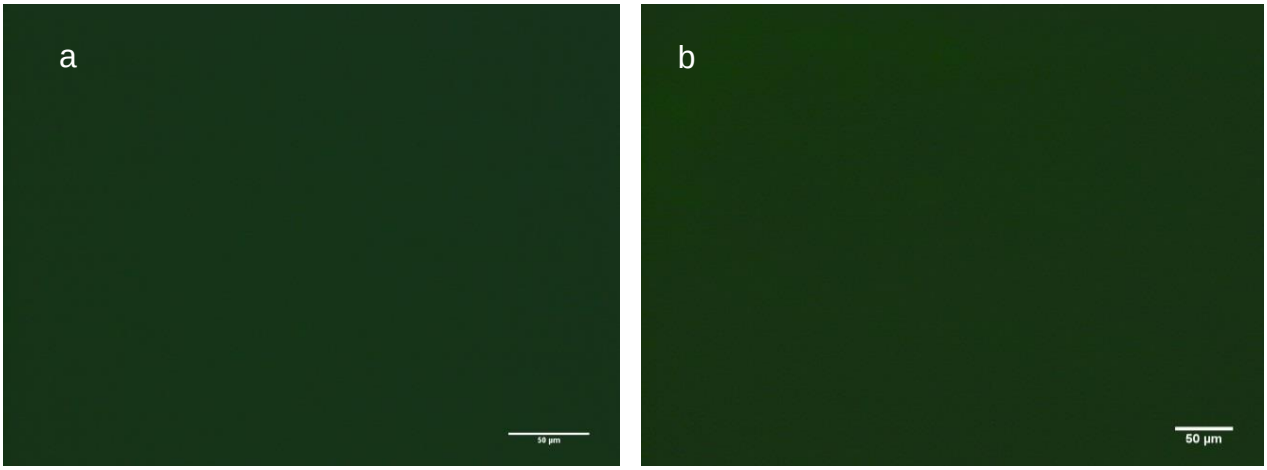

Figure 3.18: Ti6Al4V surface coated with minTBPE8 but with different surface pre-treatment: a) carbide paper polished Ti6Al4V, b) hydrogen peroxide treated.

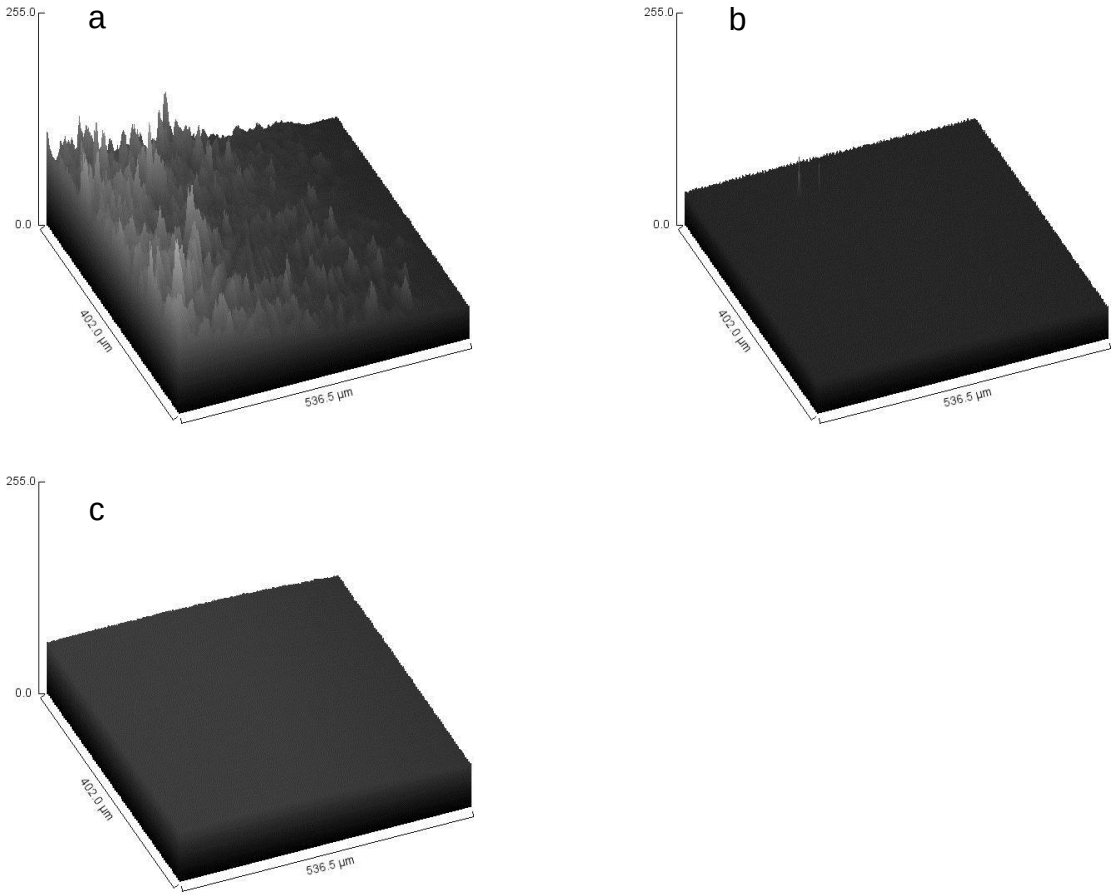

Figure 3.19: Grey value distribution of minTBPE8 peptide coated on the surface of a) mirror finish polished Ti6Al4V, b) carbide paper polished Ti6Al4V and c) hydrogen peroxide pre-treated Ti6Al4V.

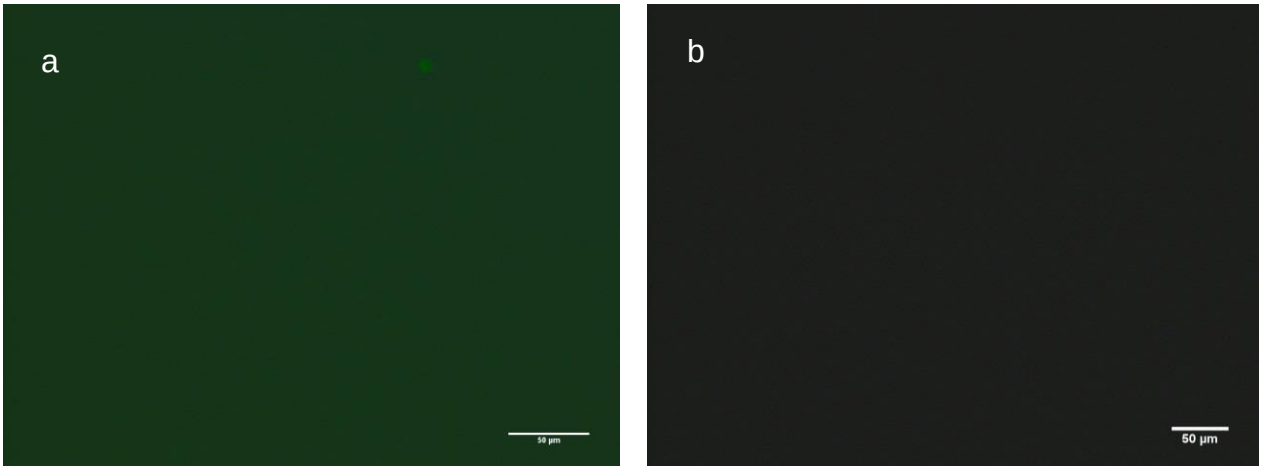

Figure 3.20: Ti6Al4V surface coated with E8minTBP but with different surface pre-treatment: a) carbide paper polished Ti6Al4V, b) hydrogen peroxide treated.

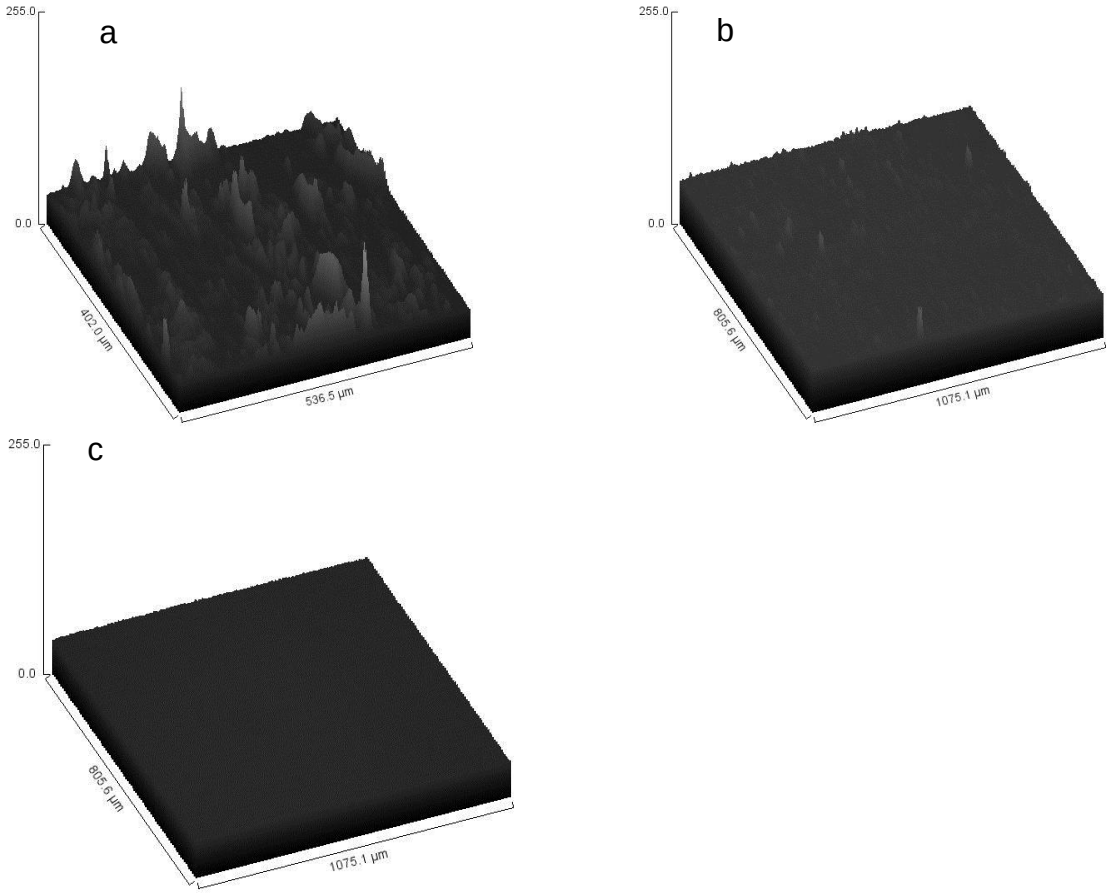

Figure 3.21: Grey value distribution of E8minTBP peptide coated on the surface of a) mirror finish polished Ti6Al4V, b) carbide paper polished Ti6Al4V and c) hydrogen peroxide pre-treated Ti6Al4V.

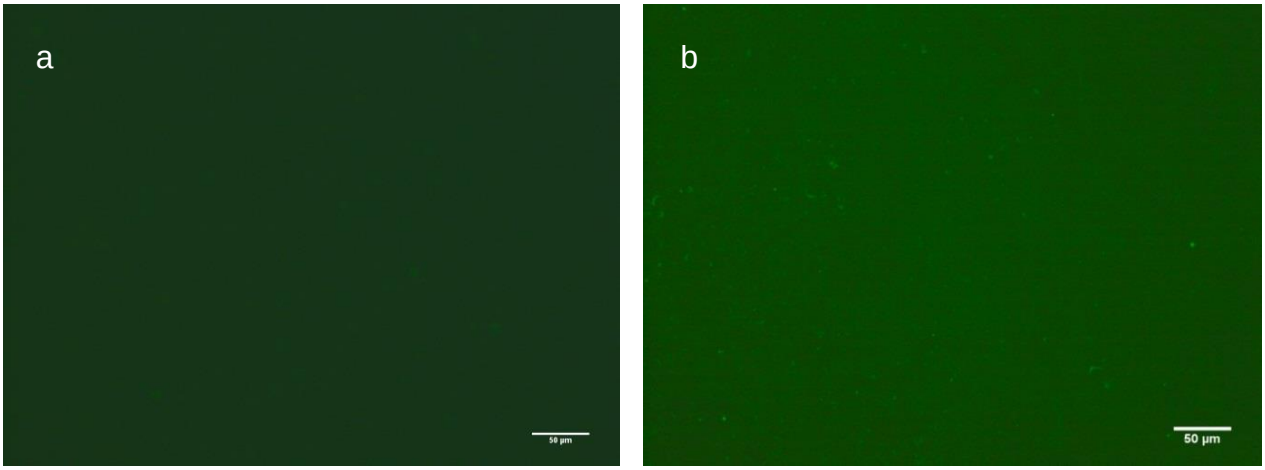

Figure 3.22: Ti6Al4V surface coated with minTBPminTBP but with different surface pre-treatment: a) carbide paper polished Ti6Al4V, b) hydrogen peroxide treated.

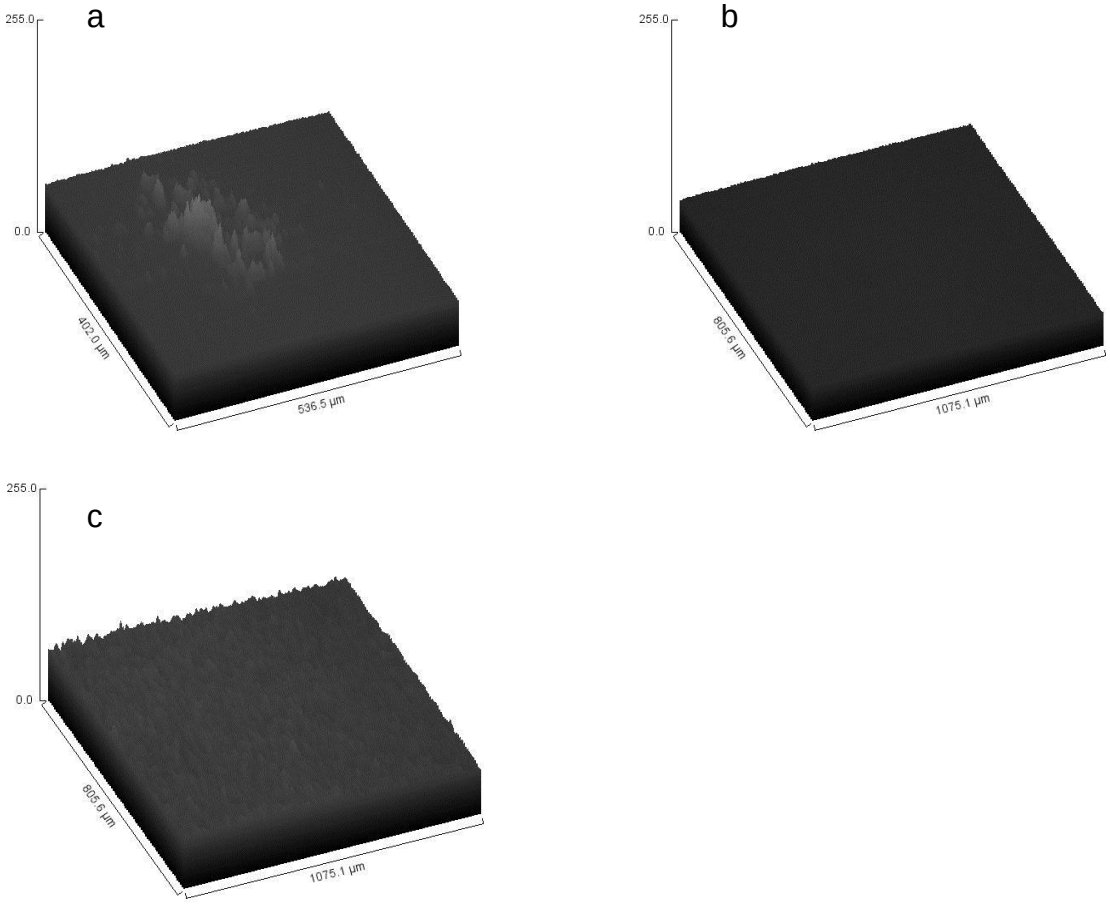

Figure 3.23: Grey value distribution of minTBPminTBP peptide coated on the surface of a) mirror finish polished Ti6Al4V, b) carbide paper polished Ti6Al4V and c) hydrogen peroxide pre-treated Ti6Al4V.

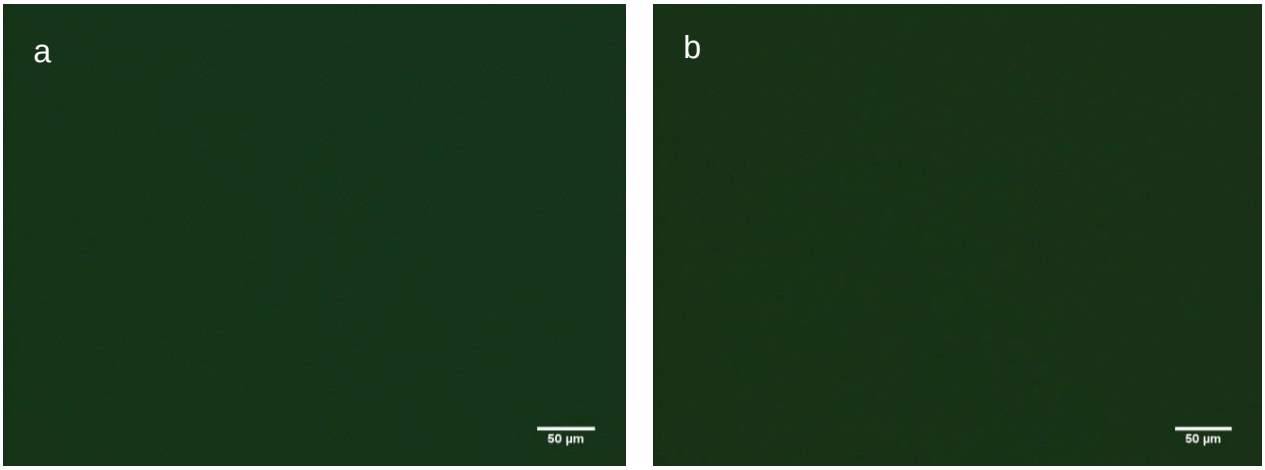

Figure 3.24: Ti6Al4V surface coated with minTBPminTBPE8 but with different surface pre-treatment: a) carbide paper polished Ti6Al4V, b) hydrogen peroxide treated.

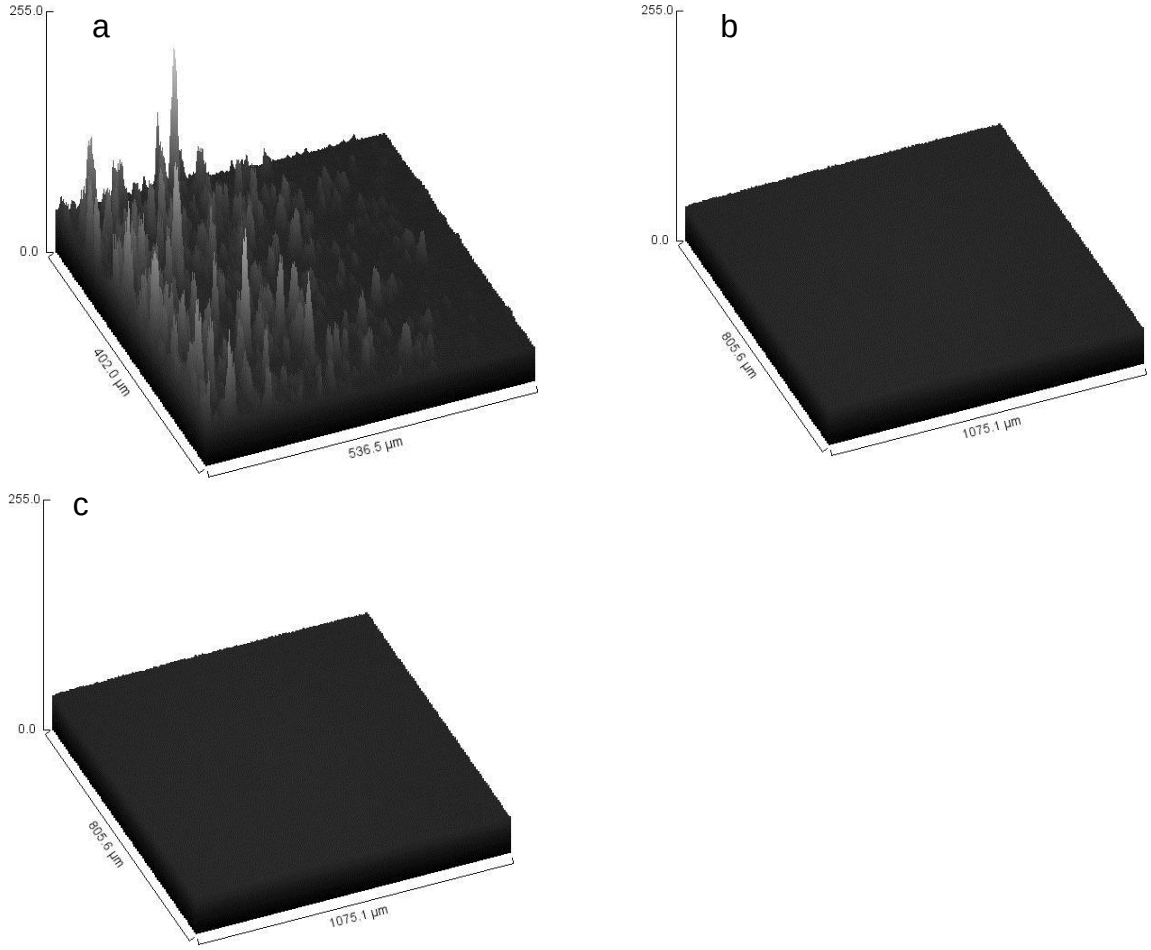

Figure 3.25: Grey value distribution of minTBPminTBPE8 peptide coated on the surface of a) mirror finish polished Ti6Al4V, b) carbide paper polished Ti6Al4V and c) hydrogen peroxide pre-treated Ti6Al4V.

The aggregates of peptide, which were observed for the surface of titanium polished to mirror finish, were not observed on Ti6Al4V polished with carbide paper 400 grit polished or on peroxide treated titanium alloy substrate.

Intensity grey values do not differ significantly between one peptide sequence and another with the exception of minTBP which intensity is twice as large as the rest of the peptides. (Figure 3.26)

Hydrogen peroxide treated titanium alloy on the other hand shows that the greatest intensity for the minTBPminTBP peptide followed by minTBP alone. The minTBPE8 and minTBPminTBPE8 showed similar values of the intensity. The intensity of E8minTBP on the surface of hydrogen peroxide treated Ti6Al4V is not significantly different than the one of a buffer which means that there was no peptide coating present.

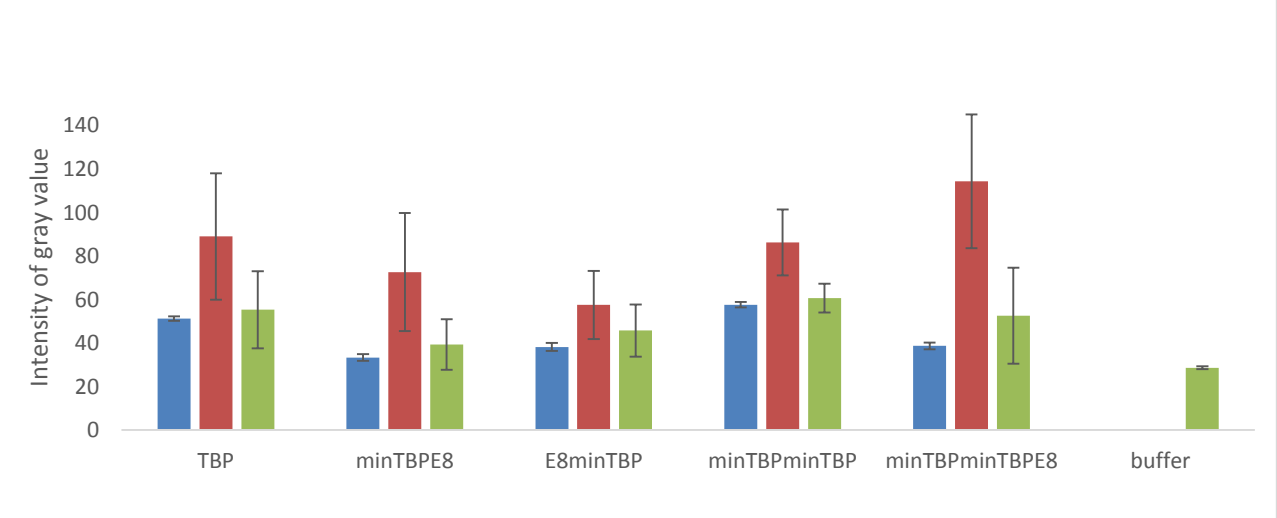

Figure 3.26: Surface of Ti6Al4V coated with peptide: blue – mirror finish polished, red carbide paper polished, and green – hydrogen peroxide treated, n = 3.

3.4 *Release of peptides from HAP and Ti6Al4V surfaces at different temperatures*

The amount of peptide released from surfaces of HAP or Ti6Al4V into the solution were analysed at three different temperatures 24 ^{o}C, 37 ^{o}C, and 44 ^{o}C but with a constant pH 7.4. These three temperatures are similar to those experienced in the body during post-surgery conditions such as elevated temperature during infection and healing process.[49]

3.4.1 Temperature dependent release of peptides from the surface of HAP

Release patterns of peptide sequences from the surface of HAP at three different temperatures are shown in Figure 3.27. The rate of the release of the peptides is summarized in the Table 3.3.

Table 3.3: Release rate of peptides from the surface of hydroxyapatite at different temperatures, n = 3.

Peptide sequence	Rate of release at 24 ^{O}C [units/s]	Rate of release at 37 ^{O}C [units/s]	Rate of release at 44 ^{O}C [units/s]
E8	(2.12 ± 0.05) x 10^{-5}	(3.65 ± 0.06) x 10^{-5}	(3.26 ± 0.06) x 10^{-5}
minTBPE8	(3.74 ± 0.08) x 10^{-5}	(4.27 ± 0.04) x 10^{-5}	(4.38 ± 0.04) x 10^{-5}
E8minTBP	(3.74 ± 0.07) x 10^{-5}	(4.27 ± 0.05) x 10^{-5}	(3.26 ± 0.05) x 10^{-5}
minTBPminTBPE8	(2.82 ± 0.06) x 10^{-5}	(3.61 ± 0.06) x 10^{-5}	(4.48 ± 0.05) x 10^{-5}

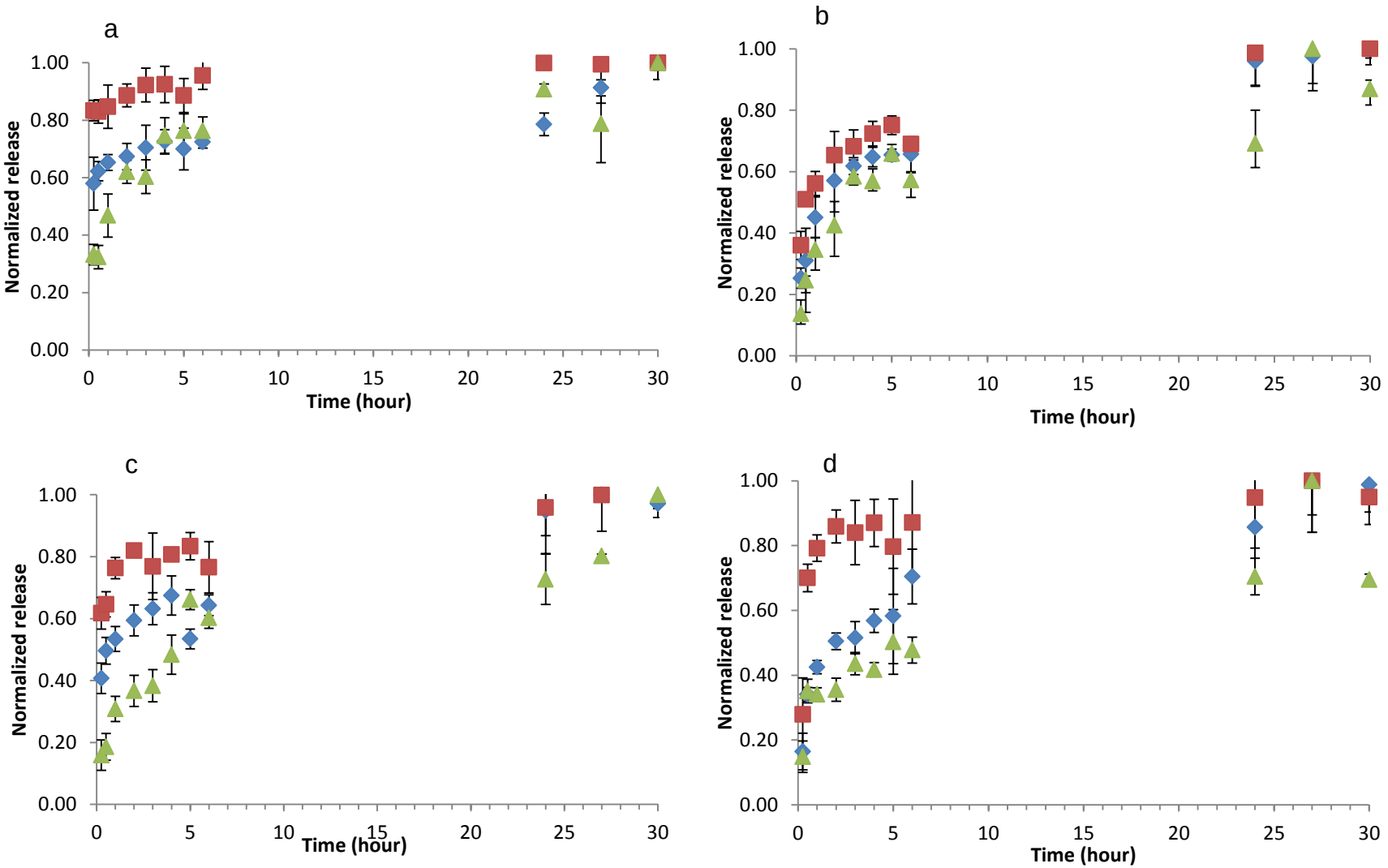

Figure 3.27: Release of peptide sequences from the surface of HAP at 24 °C (blue) , 37 °C (green) and 44 °C (red); a) E8, b) minTBPE8, c) E8minTBP, d)minTBPminTBPE8. Error bars designate standard deviation for n = 3.

3.4.2 Temperature dependent release of peptides from the surface of Ti6Al4V.

Release patterns of peptides from the surface of Ti6Al4V at temperatures: 24 ^{o}C, 37 ^{o}C and 44 ^{o}C are summarized in Figure 3.28. The rates of release for the studied peptides are summarized in Table 3.4.

Table 3.4: Release of peptides from the surface of Ti6Al4V at different temperatures, n = 3.

Peptide	**Rate of release at 24 ^{O}C [units/s]**	**Rate of release at 37 ^{O}C [units/s]**	**Rate of release at 44 ^{O}C [units/s]**
minTBP	$2.02 \pm 0.06 \times 10^{-5}$	$4.97 \pm 0.07 \times 10^{-5}$	$2.85 \pm 0.06 \times 10^{-5}$
minTBPE8	$0.83 \pm 0.07 \times 10^{-5}$	$4.50 \pm 0.04 \times 10^{-5}$	$4.05 \pm 0.05 \times 10^{-5}$
E8minTBP	$1.70 \pm 0.06 \times 10^{-5}$	$3.91 \pm 0.07 \times 10^{-5}$	$1.37 \pm 0.07 \times 10^{-5}$
minTBPminTBPE8	$2.75 \pm 0.05 \times 10^{-5}$	$3.72 \pm 0.05 \times 10^{-5}$	$0.71 \pm 0.05 \times 10^{-5}$
minTBPminTBP	$3.06 \pm 0.04 \times 10^{-5}$	$4.60 \pm 0.06 \times 10^{-5}$	$4.66 \pm 0.06 \times 10^{-5}$

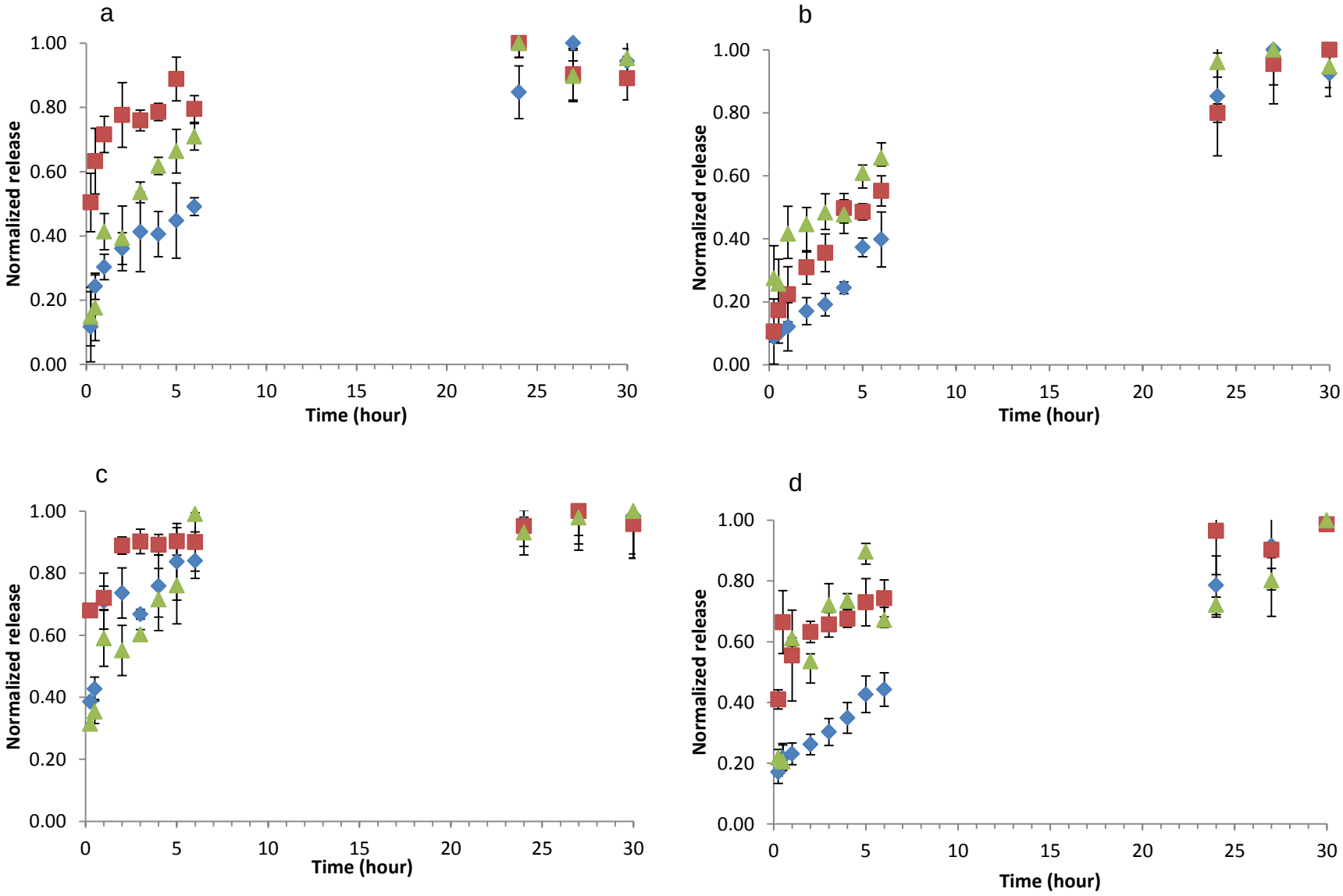

Figure 3.28: Release of peptide sequences from the surface of Ti6Al4V at 24 °C (blue), 37 °C (green) and 44 °C (red), a) minTBP, b) minTBPE8, c) E8minTBP, d)minTBPminTBPE8, e) minTBPminTBP. Error bars designate standard deviation for n = 3.

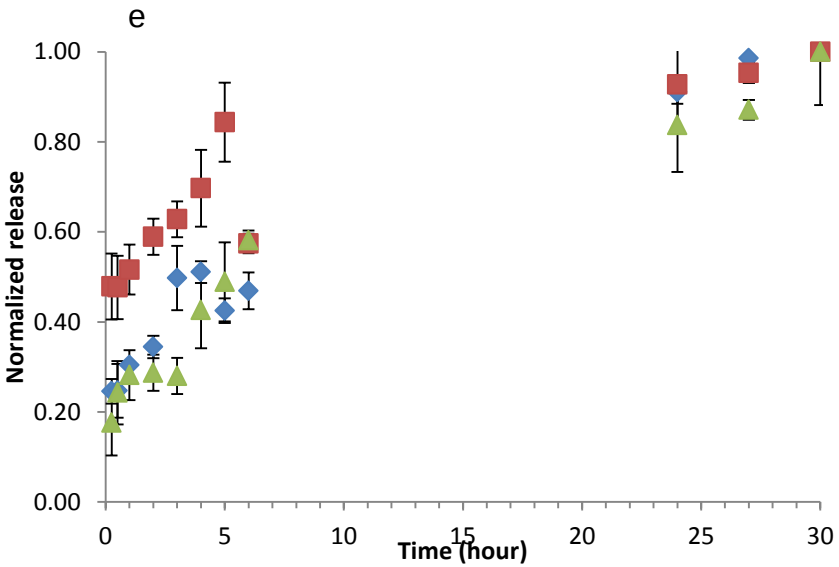

Figure 3.28 Continuation: Release of peptide sequences from the surface of Ti6Al4V at 24 °C (blue), 37 °C (green) and 44 °C (red), a) minTBP, b) minTBPE8, c) E8minTBP, d)minTBPminTBPE8, e) minTBPminTBP. Error bars designate standard deviation for n = 3.

.

3.5 *Release studies of the peptides from surfaces of HAP and Ti6Al4V at different pH values*

The influence on how fast studied peptide molecules are released from the surfaces of Ti6Al4V and HAP at different pH values was tested at the same temperature (37 ^{o}C). The pH values 5.2, 7.4 and 10.0 were chosen to mimic body conditions during the process of post-surgical trauma.[49]

3.5.1 Release studies of peptides from surface on HAP at different pH values.

Release pattern of peptides from the surface of HAP at pH values: 5.2, 7.4 and 10.0 is shown in . The rates of the release of the studied peptides from the surface of HAPV are summarized in Table 3.5.

Table 3.5: Release of peptides from the surface of HAP at pH 5.2, 7.4 and 10.0,n = 3.

Peptide sequence	**Release rate at pH 5.2 [units/s]**	**Release rate at pH 7.4 [units/s]**
E8	$(3.59 \pm 0.06) \times 10^{-5}$	$(4.08 \pm 0.05) \times 10^{-5}$
minTBPE8	$(4.24 \pm 0.06) \times 10^{-5}$	$(4.11 \pm 0.04) \times 10^{-5}$
E8minTBP	$(4.41 \pm 0.08) \times 10^{-5}$	(5.09 ± 0.04) x 10-5
minTBPminTBPE8	$(3.58 \pm 0.06) \times 10^{-6}$	$(3.54 \pm 0.08) \times 10^{-5}$

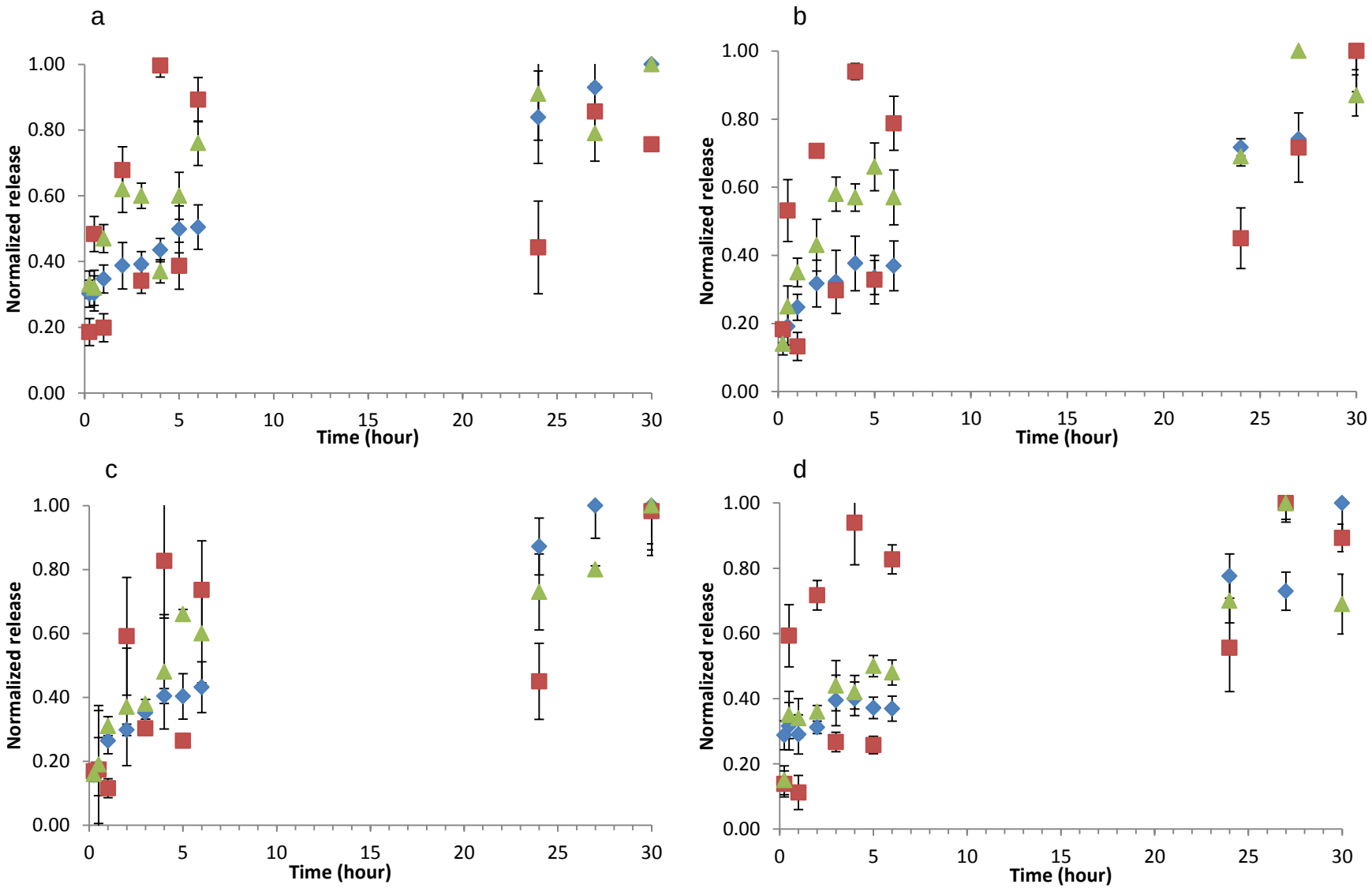

Figure 3.29: Release peptide sequences from the surface of HAP at pH of 5.2 (red), 7.4 (green) and 10.0 (blue); a) E8, b) minTBPE8, c) E8minTBP, d) minTBPminTBPE8. Error bars designate standard deviation for n = 3.

3.5.1 Release studies of the peptides from the surface of Ti6Al4V at different pH values

Release pattern of peptides from the surface of Ti6Al4V at pH values: 5.2, 7.4 and 10.0 is shown in . The rates of the release of the studied peptides from the surface of Ti6Al4V are summarized in .

Table 3.6: Release of peptides from the surface of Ti6Al4V mirror finish polished plates at pH 5.2, 7.4 and 10.0 values, n = 3.

Peptide sequence	Release rate at pH 5.2 [units/s]	Release rate at pH 7.4 [units/s]	Release rate pH 10.0 [units/s]
minTBP	$(4.96 \pm 0.07) \times 10^{-5}$	$(4.14 \pm 0.04) \times 10^{-5}$	$(1.06 \pm 0.06) \times 10^{-5}$
minTBPminTBP	$(4.60 \pm 0.06) \times 10^{-5}$	$(2.14 \pm 0.04) \times 10^{-5}$	$(1.35 \pm 0.07) \times 10^{-5}$
minTBPE8	$(3.95 \pm 0.06) \times 10^{-5}$	$(2.73 \pm 0.07) \times 10^{-5}$	$(1.06 \pm 0.06) \times 10^{-5}$
E8minTBP	$(3.94 \pm 0.08) \times 10^{-5}$	$(2.71 \pm 0.04) \times 10^{-5}$	$(2.43 \pm 0.05) \times 10^{-5}$
minTBPminTBPE8	$(3.69 \pm 0.06) \times 10^{-5}$	$(2.72 \pm 0.06) \times 10^{-5}$	$(1.35 \pm 0.05) \times 10^{-5}$

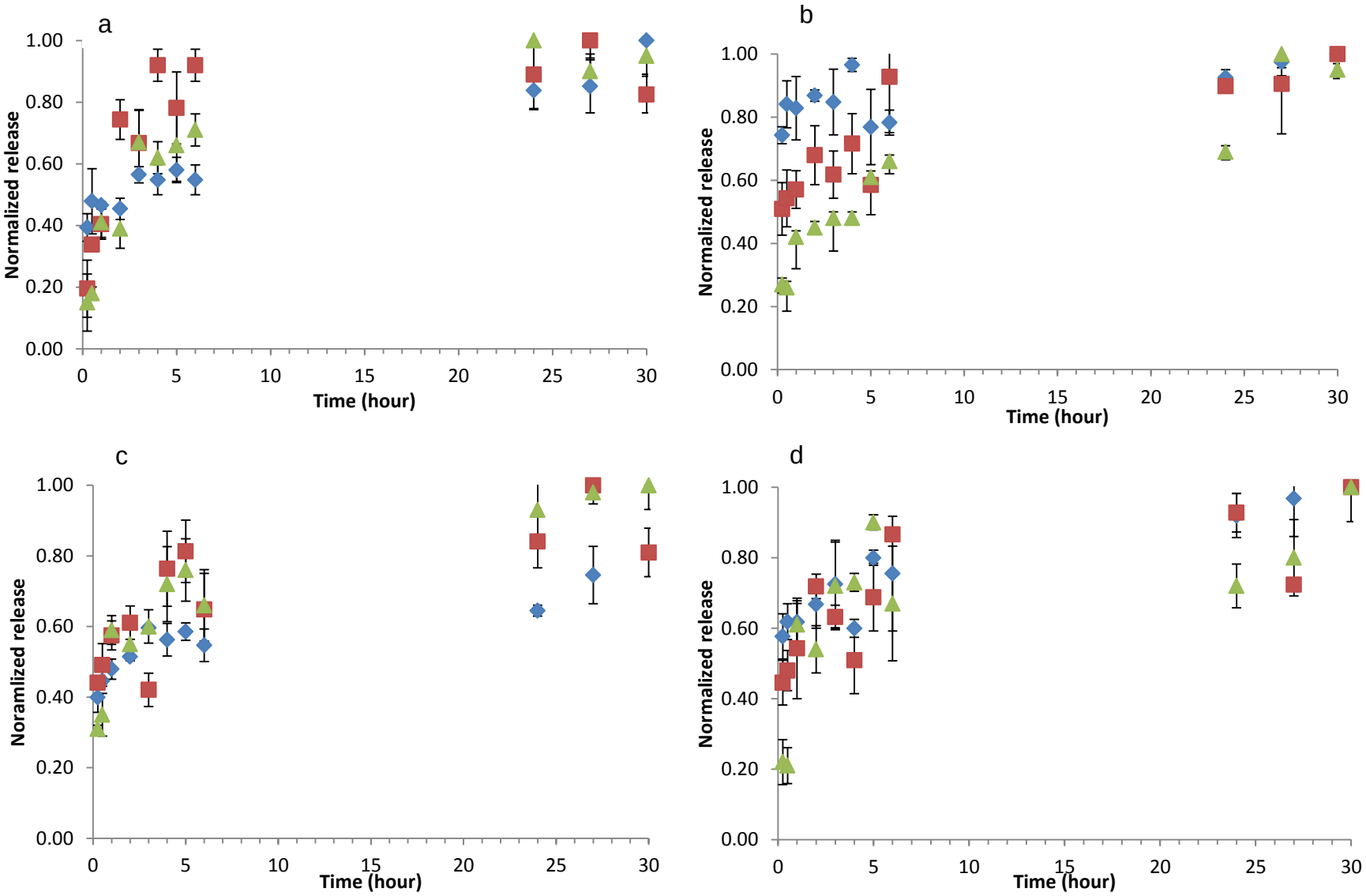

Figure 3.30: Release of peptide sequences from the surface of Ti6Al4V at pH 5.2 (green), 7.4 (red) and 10.0 (blue); a) minTBP, b) minTBPE8, c) E8minTBP, d) minTBPminTBPE8, e) minTBPminTBP. Error bars designate standard deviation for n = 3.

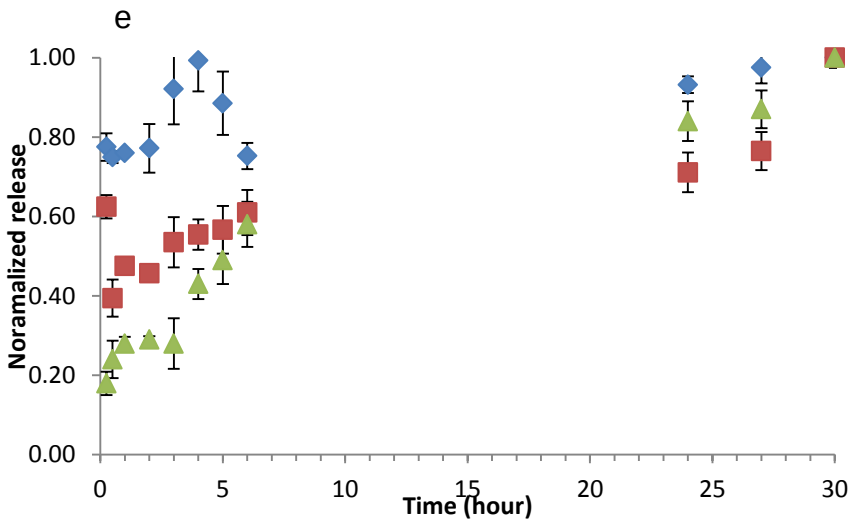

: Continuation: Release of peptide sequences from the surface of Ti6Al4V at pH 5.2 (green), 7.4 (red) and 10.0 (blue); a) minTBP, b) minTBPE8, c) E8minTBP, d) minTBPminTBPE8, e) minTBPminTBP. Error bars designate standard deviation for n = 3.

Chapter 4

4. Discussion

4.1 *Solid Phase Peptide Synthesis*

4.1.1 Purity of the Solid Phase Peptide Synthesis

The Fmoc protection group as well as the resin allow for the SPPS to give high purity of the sequence as well as good overall yield. Considering that the purity of the purchased amino acids is >98%, it can be assumed that the yield of each coupling step is at least 0.98 and the final theoretical purity of the product should be at least 0.98^x where x is the amount of amino acids in the sequence. For example, the theoretical purity for the 6-amino acid peptide sequence should be 88% whereas for 8-amino acid peptide sequence the theoretical purity of the product should be 85% and 9-amino acid peptides theoretical purity should be 83% and for 17-amino acid peptide sequence the theoretical purity should be 71%.

Purity of the peptides synthesized in this research was as expected dependant on the length of the sequence. Products of longer sequences were less pure than the one of the shorter sequences (see Table 3.1).

4.2 *Fluorescence microscopy of the FITC labelled peptides coated on the surfaces of HAP and Ti6Al4V.*

As described earlier, peptide aptamers are able to establish electrostatic interactions with inorganic surfaces. In this research peptides which bind to the surfaces of HAP and titanium were observed on the surfaces of this calcium phosphate and of

titanium alloy as designed. The peptides were designed in different N and C terminal arrangement as the presence of one or another end might influence adhesion. The peptide containing two titanium binding sequences was also used as double in the sequence as multiplicity might increase binding of the peptide molecules to the titanium surface.

One of the common techniques to prove that the surface of inorganic substrate is coated with the peptide molecules is to label the biomolecules with the fluorochrome such as FITC and then observe the surface under confocal fluorescence microscope. FITC light absorption maximum is at 494 nm and its emission maximum at 521 nm. This molecule is orange in colour in the visible light and it emits green fluorescence light when subjected to the UV light illumination of in example fluorescence microscope. The labelling of the biomolecule with FITC is based on establishing a covalent bond between the isothiocyanate group and an amine of either protein or peptide.

4.2.1 Fluorescence microscopy of HAP coated with FITC labelled peptides

Negatively charged proteins of ECM are able to nucleate and template hydroxyapatite formation.[1] Investigation of the sequences of these proteins led to the discovery of many peptides sequences which are able to establish electrostatic interactions with this calcium phosphate.[50] The E8 sequence is derived from the bone sialoprotein and its HAP binding ability has been widely studied and described in the literature.[23] The previous research shows that it is able to sustain its function when it is alone as well as when it is conjugated with another peptide such as RGD.[25] Our fluorescence studies are consistent with the previous finding that this sequence can

bind HAP crystals. The binding was observed for both E8 sequence alone as well as for the E8 sequences conjugated to the minTBP peptide. In this research the E8 peptide was coupled to minTBP peptide, which binds to the titanium, through both N- and C-terminus, respectively and was also used on its own as a positive control.

FITC labelled peptides: E8, minTBPE8, E8minTBP and minTBPminTBPE8 coated on HAP were proven to bind to this material by showing significant amount of fluorescence on the surface coated with the peptides in relation to the one obtained from images of buffer control. (Figure 3.1 - Figure 3.5) The images as well as grey value intensity showed uniform distribution of peptides.

The comparison of different intensities of the FITC fluorescence showed that the addition of the titanium binding peptide decreases the amount of peptide coated on the surface. This is due to lengthening the sequence gives more mobility to the peptide and because of this the molecule will bind in a lesser extent. The minTBPE8 and E8minTBP have different values which indicate that N-terminal or C-terminal location of E8 sequence has an influence on the peptides ability to bind to the HAP surface. Smaller intensities were seen for the E8 located at N-terminus which points out that presence of carboxylic acid of the C-terminal takes part in the binding to HAP.

4.2.2 Fluorescence microscopy of Ti6Al4V coated with FITC labelled peptides

Titanium is not a natural mineral found in the body so the sequences, which means that nature did not equipped the human body with a protein which would be able to serve as the binder. The minTBP peptide was found artificially as described before by Sano and Shiba.[8] This peptide sequence similarly to the E8 peptide was used as a

positive control to monitor the change of adsorption of the peptides on the titanium alloy when coupled to a HAP binding domain. FITC fluorescence has been observed using confocal microscopy for all peptide sequences: minTBP, minTBPminTBP, minTBPE8, E8minTBP and minTBPminTBPE8 peptide molecules, on the surface of mirror finish polished, carbide paper grit 400 polished and hydrogen peroxide treated Ti6Al4V. The distribution of the peptide molecules on the surface of the polished to the mirror finished titanium was not uniform while the rest of the surface treatment gave equal distribution of molecules across the surface.

In literature, it has been shown that the metallic surface has more hydrophobic character when it is smoother.[51] Peptides and proteins can be either hydrophobic or hydrophilic so the hydrophobicity of the surface can change the way they arrange when in contact. MinTBP-1 has half hydrophobic (L, P, A) and half hydrophilic (R, K, D) amino acids while E8 has only hydrophilic amino acids, the mirror finish polishing gives a very smooth and by this more hydrophobic surface. It is possible that hydrophilic amino acids, upon first contact with the hydrophobic surface, cause peptide to create clusters which are observed in this research. When the surface becomes rougher the hydrophobic character is decreased and then the peptides hydrophobic interaction with the surface is decreased and the clusters are not formed. MacDonald *et. al.* have found that the increase of the surface roughness of the commercially pure titanium decreased the amount of the attached protein such as fibronectin on the surface and that the protein was coated on these metallic substrate in form of a small compact clusters.[51] Deligianni *et. al*., observed similar pattern where fibronectin attachment to the rougher surface of Ti6Al4V (Ra = 0.874 µm) was less by 50 % than on the of the smoother

surface (Ra = 180 µm), unfortunately they did not record a distribution of this protein on the surface.[52] Fibronectin is built of greater amount of amino acids than the peptides used in this research but it is adsorbed on the surface of titanium by electrostatic interaction between its charged amino acids and the surface. This suggests that the hydrophilic character of the titanium surface created by different surface roughness might affect the behaviour of these peptides in similar manner and this is why the clusters were seen on mirror finish polished titanium but not on the carbide paper polished Ti6Al4V or hydrogen peroxide treated surface.

Formation of crystal like shapes on mirror finisher Ti6Al4V could be due to the salt formation of the peptides with the buffer solution or with the peptide itself. PBS buffer has phosphate, sodium and chloride ions which can interact with the charged peptide amino acids and would crystallize when the surface is air dried. The second possibility is that these crystals like structures are the representation of the intermolecular aggregation. The negative charges of one peptide can interact with the positive charges of the second peptide creating clusters of molecules. These clusters later on interact with the surface and as the water evaporates crystals of peptide salts are formed. Both of these possibilities should be further investigated. HAP surface as well as carbide paper polished and hydrogen peroxide treated Ti6Al4V surfaces did not show the crystallization pattern and the distribution was uniform for all of the peptides, even though on images of surface of hydrogen peroxide treated titanium alloy substrate some spherical clusters are present but they might be due to the pore formation. The peroxide surface treatment causes the surface to be porous and it is possible that the aggregates are inside of the pores and can be seen as the depth differences. The assumption that

the porous surface is changing the crystal formation can be also used for the carbide treated Ti6Al4V and hydroxyapatite.

Comparing the intensities of the clusters, the mean and the background, fluorescence show different variation between the intensities. The minTBPminTBP showed the greatest mean intensity which is an indication that this peptide is present in the greatest amount on the surface of Ti6Al4V. This would also be expected as the multiplicity of Ti binding peptide sequence domains should lead to better binding due to more sites for the binding.

The intensities of the peptides on mirror finish polished, carbide paper polished and hydrogen peroxide treated surfaces in general show no significant difference between the three treatments used with the exception of minTBP peptide on carbide paper polished surface and the E8minTBP peptide on the hydrogen peroxide treated Ti6Al4V.(Figure 3.26) In the first case the amount of molecules is twice as much as for the other surface treatment. As discussed earlier increases surface roughness changes increases the hydrophilic character of the surface, it is possible that this change affects the minTBP as it has 50 % of hydrophobic and 50 % of hydrophilic amino acid in the sequence. In the second case, intensity of the peptide coated surface does not differ significantly from the buffer treated one, which means that there is no peptide present on the surface. The change of surface chemical composition due to peroxide treatment didn’t change the interaction of other peptide sequences with the Ti6Al4V, it is possible that the amino acid binding site location become unfavourable for this particular peptide sequence. These two observations should be further investigated to fully understand the reason behind them.

Comparing the intensity of HAP and Ti6Al4V bounded FITC labelled peptides it can be noticed that the HAP has significantly greater amount of molecules on the surface (Figure 3.14). This could be explained by the fact that HAP discs produced in this research are porous and this will cause the peptide to be absorbed in greater amount then in case of titanium. This would cause molecules bound to HAP to show a greater intensity than the one on the surface of Ti6Al4V which only exposes the top layer for binding. Another explanation would be that the binding ability of the E8 peptide is much greater than the one of the minTBP. The HAP binding domain has eight glutamic acids in its sequence each of which capable of electrostatic interaction with the calcium ions, minTBP on the other hand is known to use only arginine and aspartic acid to establish bonding and they use localized charges at a specific location on the surface. The difference in amount of binding sites and the specificity of target suggests that the E8 peptide would establish stronger binding than minTBP does, causing the observed amount of peptides on the HAP to be much greater than the one on Ti6Al4V.

It can be observed that two additional minTBP peptides significantly decrease the binding of this molecule on the surface of HAP, while increasing its binding on titanium as intended. This is due to the fact that there is only one HAP binding domain in the longest peptide and the additional weight and molecular mobility caused by the conjugation of other domain, leads to a loss in stability of the binding and weaker adsorption on the surface. On the other hand the minTBPminTBPE8 binding domain amount increases making it more stable on the surface of titanium. The multiplicity of the minTBP and the strengthening of its binding have been already observed by Kashiwagi *et. al*. In his research he encoded one two and three minTBP on the BMP-1

protein and found that with the amplifying of number of this peptide the binding of this protein to titanium surface was strengthened.[18]

4.3 *Release of peptides at different temperatures and pH conditions*

Average body temperature is 37 ^{o}C. However during infections body temperature is very often higher which is a natural defence mechanism of organism against microbes [49]. Temperatures measured close to the skin on the other hand can be a couple of degrees lower than the inner temperature as it is in constant contact with the temperature of an environment [49]. It is well known that under higher temperatures molecules show more movement than at lower ones.[53] When the peptide is electrostatically attached on the surface of inorganic material the movements of the molecule will cause it release. The more movement there is the sooner the peptide will detach from the surface so increase in the temperature should lead to increase in the molecules release. Many research groups are focusing on the thermally responsive peptides for drug delivery as small shift of temperature can change the interactions between the peptide molecules, drug transported and the surface on which they are attached.[28, 54-56]

Similarly to the temperature variation the pH values can differ in the body. After surgery the pH of the wound can be changed due to the trauma. pH at implant insertion site can drop to as low as the and can be elevated to around 10 when the immune system is fighting the bacterial infection.[49] These acidic and alkaline conditions can change the behaviour of inorganic materials inserted in to the body as well as of the

biomolecules, which coat them. It is well known that the HAP is stable above pH 7.4. [57] However, when the pH is lowered the HAP begins to change into other forms of calcium phosphate such as brushite and it starts too dissolute.[58]

Metals on the other hand can begin to corrode under acidic conditions. Titanium has a very good resistance to the corrosion because it develops a passivation layer. The new formed layer of oxide prevents it from dissolving. [48, 59] In aqueous solutions the titanium top passivation layer is modified to form titanium hydroxide groups which can later weakly react with water molecules creating a positively and negatively charged hydro-complexes.[48] The change in positive and negative units on the surface can have an influence on the electrostatic binding of biomolecules. The pH changes the protonated and deprotonated state of peptides, which may perturb or enhance electrostatic interactions. PKa values of the amino acids side chains of peptides designed for this research are summarized in Table 4.1.

Table 4.1: pKas of the amino acids side chain groups found in minTBP and E8 sequences.

Amino acid	**Amino acid pKa of side chain**
Aspartic acid, D	3.9
Glutamic acid, E	4.1
Lysine, K	10.7
Arginine, R	12.5

The conditions which were designed in this research are pH of 5.2, 7.4 and 10.0. This pH values do not cross the bounders of the charged state of any of the amino acids present and should not affect the peptide binding.

In this research release of all of the peptides from both HAP and Ti6Al4V at all tested conditions, showed very rapid release rate right after the immersion of the peptide coated surface in the buffer solution. After 2-3 hours the rate of the release slows down and small changes were observed. (Figure 3.27 - Figure 3.29) The only exception is the release of the peptide from HAP at pH 5.2 and it is discussed later in the Section 4.3.4. The release rate of the peptide from the surface was previously shown by Culpepper *et. al*. in their release study of E2DGEA, E4DGEA, E7DGEA and DGEA sequence from the allograft bone material.[60, 61] In their research they also observed rapid release of the peptides from the allograft particles which slowed down after 6 hours of study. They found that the oligoglutamic acid sequence containing peptides were retained on the surface of the allograft particles for 5 days while immersed in TBS, pH 7.4 and kept at 37 ^{O}C. In addition they also found that the DGEA sequence, which does not have the specific binding ability to calcium phosphate was completely released after 24 h.[61] This suggests that the peptide might be retained on the surface of the inorganic material if it has a specific binding ability towards this material for longer period of time than when material non-specific peptide is used. In our research neither the surface of HAP nor the surface of Ti6Al4V was tested for fluorescence after the release study was performed so it is impossible to state if the peptide was fully release or if some fraction of the peptide was retained on the surface. These needs to be considered in the future by performing fluorescence imaging of peptide coated inorganic materials, which were previously immersed in the solution for minimum of 24 hours.

4.3.1 Release of peptides from the surface of HAP at different temperatures

The release of peptides from the surface of HAP increases with increased temperature is summarized in the Table 3.3. There is a slight error in the measurements at 44 ^{o}C where by a mistake the temperature was raised between 4 and 5 h of measurements to 60 ^{o}C for 15 minutes. This change is reflected by the increase of release at 5 and 6 h measurements. The rate presented here is based on the first 4 hours of measurements and might not be accurate as the amount of data points is based on five data points.

For all of the peptides the release of molecules from the surface of HAP at 24 ^{O}C was always slower than the one for 37 ^{O}C. (see Table 3.3) This would be expected as temperature increase causes increase of the molecular movements which might further result in weakening of the electrostatic interaction with the surface. The rate of release at 44 ^{O}C was observed to be faster for minTBPE8 and minTBPminTBPE8 peptide sequences, which was expected. The release of E8 and E8minTBP molecules at 44 ^{O}C was not faster at higher temperature but this could be a result of the smaller data polls used to calculate the rates.

The comparison of the rate of release for studied peptide sequences at 24 ^{o}C and 37 ^{o}C were observed to be significantly faster for the minTBPE8 and E8minTBP than for the E8 and minTBPminTBPE8. This difference suggests that one minTBP conjugated with E8 have weakened the interaction of the E8 with the surface of HAP. The weakening of peptide and surface interaction due to the attachment of another molecule was earlier reported by Fujisawa.[62] What is interesting minTBPminTBPE8 peptide

molecules, which contain two titanium binding domains, were released much slower than minTBPE8 and E8minTBP. MinTBP has a negatively aspartic acid in its sequence, Asp was previously shown to bind HAP but it interaction is weaker than the one of the Glu.[63] This suggests that there might be some interaction between the charged amino acid of minTBP with the HAP and that the proximity of the charges with the surface is favourable only when the titanium binding domain is in a specific distance from the HAP binding domain. The spatial arrangement of the peptide in relation to the surface was earlier observed to be an important factor of the peptide – surface interaction as when the molecule is not in a specific conformation the charges of amino acids will not be in a good proximity to the surface and the electrostatic interaction of peptide-surface will be limited.[11, 64] The not favourable arrangement of the Asp with the relation of the surface would explain why minTBPminTBPE8 have much more stable interaction in comparison to minTBPE8 and E8minTBP as another binding site is introduced for the longer molecule.

The rate of release at 44 ^{O}C between the different peptide molecules is not consistent with the observation at the 24^{o}C and 37 ^{o}C. The inconsistency can be caused by the error introduced while performing the test.

4.3.2 Release of peptides from the surface of Ti6Al4V at different temperatures

For all of the peptides the release of molecules from the surface of Ti6Al4V at 24 ^{O}C was always slower than the one for 37 ^{O}C. (see Table 3.4) This observation would be expected as temperature increase causes increase of the molecular movements which might further result in weakening of the electrostatic interaction with the surface. The

rate of release at 44 ^{O}C was observed to be the fastest only for the minTBPminTBP sequence. It was observed that for minTBPminTBPE8 and E8minTBP the release at this temperature was the slowest while for minTBP and minTBPE8 it was second slowest. This observation can be due to the earlier discussed error introduced in the measurements.

The comparison of the release rate between peptide sequences three tested temperatures does not show a unique pattern for the molecules such as the one observed for surface of HAP.

At 24 ^{O}C the rate of release from the slowest to the fastest was observed as follows:

minTBPE8 < E8minTBP < minTBP < minTBPminTBPE8 < minTBPminTBP

At 37 ^{O}C the rate of release from the slowest to the fastest was observed as follows:

minTBPminTBPE8 < E8minTBP < minTBPE8 < minTBPminTBP < minTBP.

At 44 ^{O}C the rate of release from the slowest to the fastest was observed as follows:

minTBPminTBPE8 < E8minTBP < minTBP< minTBPE8 < minTBPminTBP.

The titanium surface pH value have been reported to have more acidic character even though the positively charged hydro-complexes are present on the surface in aqueous solution,[30, 48, 65] this suggest that the surface of Ti6Al4V should repel negatively charged glutamic acids, leading to faster release of E8 containing peptides. This suggests that the minTBP and minTBPminTBP should bind to the surface the strongest and be released with the slowest rate.

Release pattern of the molecules, which have different motifs at C and N terminals, shows that stability of the peptide on the surface depends on the termini location of E8 and minTBP. At 24^{o}C the release of minTBPE8 was higher while for the rest of

temperatures was slower release. This change in behaviour should be investigated. At 24 ^{o}C the fastest release is recorded for minTBPminTBP and minTBPminTBPE8, which is interesting as these peptides have two titanium binding domains and in theory should bind the strongest on the surface of Ti6Al4V. At 37 ^{o}C release of the minTBPminTBPE8 molecule is the slowest while the minTBPminTBP is still released faster than the rest of peptide sequences. At 44 ^{o}C the release of minTBPminTBPE8 is the slowest while the one of minTBPminTBP is the fastest. The multiplicity of the peptide has previously been proven to increase the binding ability of the sequence by Kashiwagi *et. al*. who showed that three minTBP peptides fused with Bone Morphological Protein significantly increase the binding in comparison with one.[18] Also in their studies of the different length oligoglutamic acid Culpepper *et. al* showed that the more repetition of the charged glutamic acid the stronger the binding is.[60] In this research his observation has been shown for the minTBPminTBPE8 with the exception of the data at 24 ^{o}C while is much different from the pattern observed for the minTBPminTBP.

4.3.3 Release of peptides from HAP at different pH conditions

As mentioned before HAP can undergo changes due to the change into a different calcium phosphate. HAP is known to be very stable at pH above 7.4 but at acidic pH, brushite which is a very soluble ceramic material, is the more stable form of calcium phosphate. This means that the calcium phosphate will slowly degenerate under acidic conditions.

All of the peptides had similar release rates from the surface of HAP at both pH 7.4 and at pH 10.0. This similar rate can imply that neither calcium phosphate nor the

peptides electrostatic binding properties were changed due to the different pH (Table 3.5).

At pH of 5.2 on the other hand, the concentration of released peptides was fluctuating from high to low values (see Figure 3.29). This change in the concentration of fluorescent molecules in the solution is observed for all of the peptides released from the HAP and can be due to the change of this ceramic material into the brushite. It is possible that as brushite is being dissolved new HAP is formed leading to adhesion of peptides back on the surface of the ceramic material. BSP and its oligoglutamic peptides are known to nucleate the hydroxyapatite crystals and to mature the amorphous calcium phosphate into the HAP.[27, 66, 67] It has been proposed that the spatial arrangement of the peptide amino acids in relation to the surface is responsible for favouring HAP over other forms of calcium phosphate.[67] It is possible that the E8 domain has a preference to bind to HAP. This means that if the process of HAP to brushite transformation occurs and this calcium phosphate is dissolved together with the release of peptides, then the released biomolecules might attach back on the surface of HAP. This process should be further investigated. One possible way to research it would be by measuring the amount of calcium and phosphate released and analysing the surface of the calcium phosphate in terms of crystalline forms at a given time. This should be further related to the amount of the peptide molecules attached on the surface and released in the solution at each data point.

At pH 5.2 the molecules release rate from the most slowly released to the fastest released was observed as follows:

minTBPminTBPE8 < E8 < minTBPE8 < E8minTBP

At pH 7.4 the molecules release rate from the most slowly released to the fastest released was observed as follows:

minTBPminTBPE8 < E8 < minTBPE8 < E8minTBP

At this pH values all of the molecules exhibit the same release in relation. What is interesting the doubling of the minTBP in the sequences caused minTBPminTBPE8 to be released slower than the E8 is released while the molecules with one titanium binding domain are released faster. These observations suggest that the minTBP is able to interact with the surface of HAP but it might need a special spatial arrangement of charged molecules, as described during the temperature dependent studies, for the attachment to be favourable. Another interesting observation is that release of the minTBPE8 is slower than the release of E8minTBP. In this case the arrangement of the E8 at the N – terminal is observed to be unfavourable and causes the molecule to be released faster. This could be explained by the shielding of the surface caused by FITCconjugated to the N-termini. FITC is a very bulky molecule and because of its size it can decrease the proximity of the E8 peptide with the surface especially if the binding peptide is on the same terminal as it is attached.[68] In this research the FITC shielding effect was reduced by addition of the Ahx spacer between the peptide molecule and the fluorochrom which has been previously reported by Jullian *et. al*. but its effect is not fully overwhelmed.[68] In previous studies done by Fujisawa on the molecules involving E7 sequence at the N – terminal the FITC labelled molecules did not exhibit significant difference than the one without the label.[62] This might suggest that the E8 peptide is more affective binder at the C – terminal. If this is the case then it can be assumed that

the carboxylic acid at the terminal also takes part in the binding with HAP. This binding of the carboxylic terminal have been previously proposed by Roddick-Lanzilotta in his study of the glutamic acid attachment to the titanium. [10]

4.3.4 Release of peptides from Ti6Al4V at different pH conditions

The dissociation of the peptides form the Ti6Al4V shows a trend where in the acidic conditions all of the peptides dissociated much faster from the surface than in alkaline (Table 3.5).

In aqueous solutions titanium top passivation layer is modified to form titanium hydroxide groups which can later weakly react with the water molecules creating positively and negatively hydro-complexes of titanium. [48]

$$Ti\text{-}OH + H_2O \Leftrightarrow [Ti\text{-}O]^- + H_3O^+$$

$$Ti\text{-}OH + H_2O \Leftrightarrow [Ti\text{-}(OH_2)]^+ + OH^-$$

These charged hydro-groups are sites for electrostatic interaction of arginine and aspartic acid of minTBP,[25] which means that changing the amount of the hydroxide sites should alter the binding properties of the peptide and be directly related to the release of them from the surface. It has been reported that placing titanium in alkaline solution increases the amount of hydroxylated titanium as well as it will lead to production of greater amount of negatively charged hydrates.[48] The acidic conditions on the other hand lead to a decrease of the hydro-complexes by leaving only the uncharged oxide layer.[48] In our research the release rate of peptides was decreased as the pH value was increased, which is interesting result as the surface of titanium should become more negatively charged and should repell the negatively charged glutamic acid and aspartic acid. On the other hand the interaction of arginine with the

Ti6Al4V surface should be strengthened at alkaline conditions which might result in more stable binding and slower release. The pH change and the binding of positively charged amino acid: lysine was studied by the Roddick-Lanzilotta *et. al*.[9] In their research they found that the alkaline conditions does not change significantly the titanium binding ability of lysine till the pH value reaches its pKa value where this amino acid is fully deprotonated, but the change of the titanium surface charge did not affect the molecule interaction significantly.[9] The reason for our finding is not well understood and needs to be further investigated.

At pH 5.2 the molecules release rate order from the most slowly released to the fastest released was observed as follows:

minTBPminTBPE8 < E8minTBP ≤ minTBPE8 < minTBPminTBP < minTBP

At pH 7.4 the molecules release rate order from the most slowly released to the fastest released was observed as follows:

minTBPminTBP < E8minTBP ≤ minTBPminTBPE8 ≤ minTBPE8 < minTBP

At pH 10.0 the molecules release rate order from the most slowly released to the fastest released was observed as follows:

minTBP = minTBPE8 < minTBPminTBPE8 = minTBPminTBP < E8minTBP

At pH 5.2 and 7.4 all of the molecules were released slower than the minTBP from the surface of Ti6Al4V, while at pH 10.0 minTBP was released the slowest. These could be explained by the fact that at basic pH surface of titanium has more negatively charged oxides than at acidic pH and neutral pH.[48] As the molecules with the E8 domain have more negative character than the one of the minTBP they will be released more readly than the minTBP. It is also possible that the fast release of the minTBP

peptide in relation to the E8 conjugated ones is caused by the interaction of the glutamic acid with the surface of titanium in addition to the interaction of the arginine and lysine. Roddick-Lanzilotta *et. al* have found that the glutamic acid interact with the surface at the neutral and acidic contitions.[10] If this interaction is present for our studied peptides then it is possible that the stability of molecules on surface would be increased with the addition of the glutamic acid domain and the peptides containg E8 peptide will be released slower than the minTBP.

Chapter 5

5. Conclusions and Future Work

Peptide aptamers are small biomolecules made of amino acids which have the ability to bind towards organic and inorganic materials. They can bind to different surfaces via electrostatic interactions which form under mild aqueous conditions. Merging two different motifs each possessing different function could allow for two surfaces to be connected together. The peptides designed in this research possess a function of binding to the HAP and titanium, and were proven to be able to establish electrostatic interaction with these surfaces. However aqueous solution release studies at different pH values and temperatures and temperatures showed that the nature of the binding is very weak and that these peptides will not be able to serve as an organic binder between the two inorganic layers when in the body. The peptides would be released within the first 30 hours and the coating would not induce faster integration of the molecules on the surface of an implant.

One possible way to overcome this is encoding of these sequences into proteins with multiple domains such as ferritin. This way the binding domains will exist in multiplicity and the bonding would be stronger. Another solution is to use covalent bonding between the inorganic surface and the organic peptide. Another thing which could be improved is the binding ability of minTBP. It is very weak in comparison with the strength of the E8 sequence and HAP adhesion. The titanium binding sequence should be modified or new sequence with higher affinity should be generated.

The release of the molecules from the surface of HAP showed a very interesting behaviour and the mechanism at pH 5.2 where a fluctuation of released peptide

concentration was observed. This phenomenon should be investigated by analysing the change of the crystalline form of calcium phosphate each time the amount of peptide is analysed, together with fluorescence microscopy of the HAP surface at a given data point. The release of the peptide molecules at 7.4 and 10.0 pH values showed that the location of binding domain at C or N terminal might have an effect on the release behaviour of peptides. The temperature release of the molecules from the surface of HAP and Ti6Al4V showed that most of the studied peptides are released faster at higher temperature. It has also been shown that increasing the pH value causes the release rate of peptides from the surface of Ti6Al4V to be slower.

Another interesting behaviour observed in this research was the aggregation of the crystal structures on the surface of the titanium. The reason whether the peptides are able to self-aggregate or if these peptides aggregate in crystals due to presence of buffer should also be looked at. Information of self-aggregation of biomolecules gives some more data on how the biomolecules are arranged into membranes, cells and tissues and maybe in the future use of this knowledge will allow creating artificial bone based on the peptide self-assembling and biomineralization properties.

6. Appendix

6.1 *Determination of the Secondary Structure by Circular Dichroism Spectroscopy*

Folding of the peptides into secondary structure was analysed by the Circular Dichroism Spectroscopy. All peptides were of dissolved to 100 μM concentration in the phosphate buffer pH 7.4. Peptides were measured inside the cuvette of the 1cm and 0.1cm light path length. The spectra were recorded as the comparison of the negative and positive areas at 195 nm, 212nm as well as the shape of the curves were tools to distinguish between b-sheet, a-helices and random coil conformation of peptides and proteins [39,40]. The shape of the curve recorded by the CD spectrophotometer (Figure 6.1) is consistent with the literature random coil curve shape. The values of Circular Dichroism at the wavelength around 195nm are negative and at the wavelength around 220 are positive again confirming the random coil conformation. These results are consistent for all peptides measured for both 0.1 cm and 1.0 cm light path length.

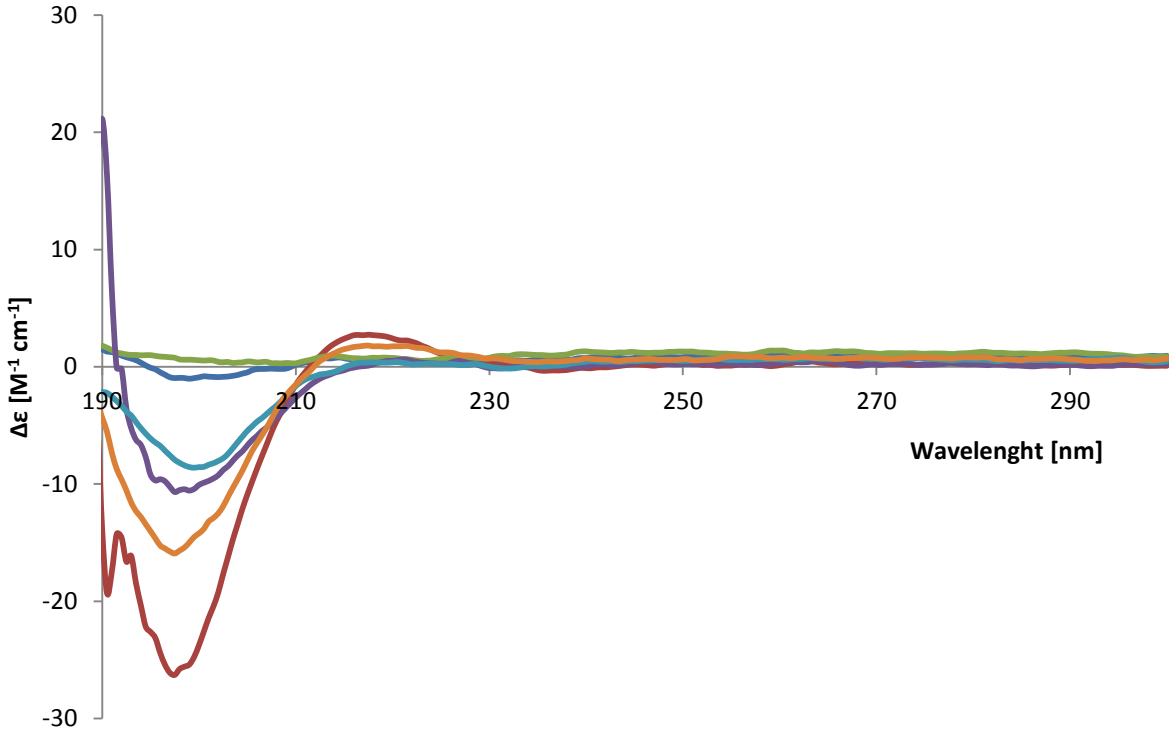

Figure 6.1: Circular Dichroism spectra of the peptides studied E8: path length 0.1cm – dark blue; path length 1.0cm- red, minTBP: 0.1cm - green, 1.0 cm – purple; minTBP-E8: 0.1 cm – light blue, 1.0cm - orange.

6.2 *Secondary Structure studies of peptide by the Circular Dichroism Spectroscopy*

Peptides aptamers use the electrostatic interactions of the charged amino acids to establish binding with the oppositely charged surfaces of inorganic and organic materials [23]. This means that the location of the charged amino acid in the peptide sequence can have a great influence on the binding with given substrate. The spatial orientation of peptides can be directed by their folding into secondary structures such as helices, sheets and random coils [27]. These structures are created when the hydrogen interactions between residues of the same or different molecules are established. The

unordered structure called random coil is the most common for the small peptides and it does not show any specific hydrogen bonding. Beta sheets are usually created when Tyr, Phe, Trp, Thr, Val, Ile are present in the peptide sequence, while the helices is observed when Met, Ala, Leu, Glu and Lys are present [69, 70] based on the amino acids residues in the sequence the E8 as well as minTBP-E8 have a propensity to adopt helical structure because they are made of the glutamic acids residues. Circular Dichroism Spectroscopy (CD) is commonly used technique to analyse if the secondary structures of peptides and proteins. In this technique light is circularly polarised, which allows to notice difference in between chiral molecules. All amino acids beside Glycine are chiral molecules and they absorb left polarized light differently than the right polarized light. This means also means that the proteins and peptides build from the amino acid will exhibit chirality, be optically active and can be analysed by the CD. It is well established that the secondary structures of peptides and proteins have distinct Molar Circular Dichroism pattern. (Figure 3.7)

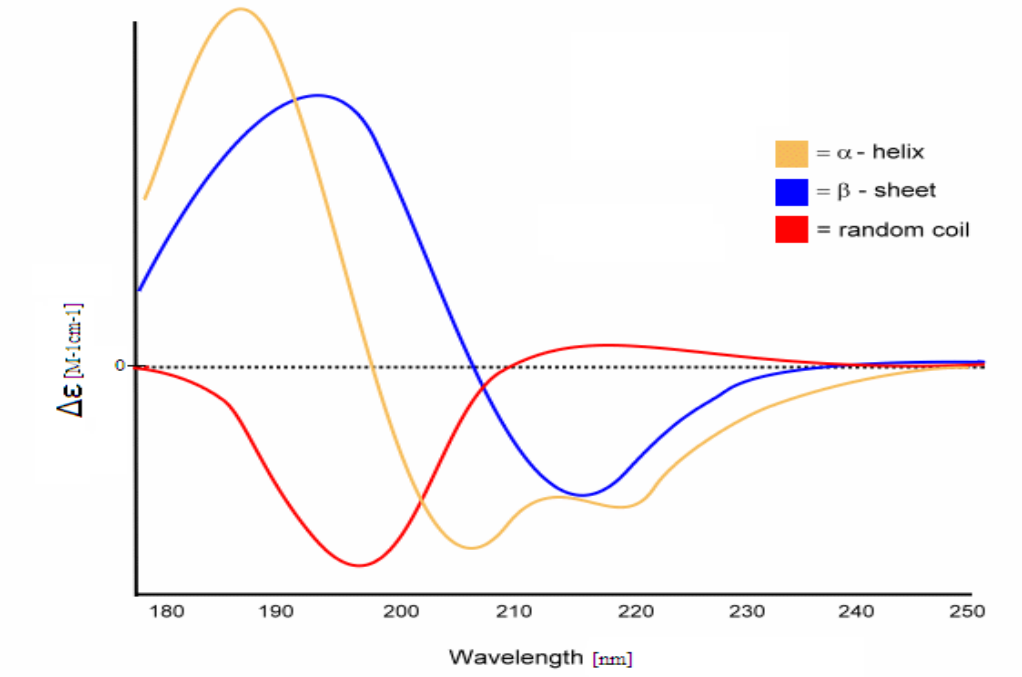

Figure 6.2: Circular Dichroism pattern of the helices - Yellow, sheet – blue and random coil – red.

The difference in the pattern is observed because secondary structures would force the amide bond to assume π or π angle. This angle will direct which electrons of amide bond will absorb the light. The amide bond absorption spectra are observed for the wavelength of around 220 nm for n -> π* and the wavelength of around 190 nm for π -> π*.

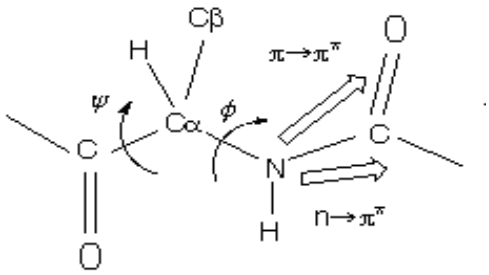

Figure 6.3: Representation of the angles of the peptide bond and the electron transition.

Analysis of the wavelengths when the transition takes place showed that the peptide assumes the random coil structure when the spectrum is positive at the n -> π* (λ≈220) and negative at π -> π * (λ≈190) [69, 70]. Peptide is in a form of B-sheet when the values at π -> π * are negative and positive n -> π [69, 70].The coupling of the excitons is observed in case of a-helices so the π -> π * transition is observed twice and the characteristic values are positive at perpendicular excitons at π -> π *, negative for parallel excitons and π -> π * and negative at n -> π * [69, 70].

The secondary structures of the peptides which were synthesised in this research were described only for the oligoGlutamic acid. The sequence of polyGlu was observed to be dependent on the pH in which it is analysed. The structure of α-helices was observed at 8.0 pH and random coil was observed at 4.0 pH [11]. Another research analysed the SpSpEEEEEEE sequence[11], which has two negatively charged phosphoSerines (Sp)

at their N-terminal conjugated to the eight consequent Glutamic acid residues. In this research formation of helices was observed in the phosphate buffer with Calcium ions at pH 7.4 and at 36 ^{o}C. The addition of the positive Calcium ions changed the ionic strength of the solution. This change could influence the arrangement of the residues in the peptide molecule and induce helices.

In this research, CD spectra of all the synthesized peptides were analysed in 100 mM, pH 7.4. The choice of pH is based on the average body pH of 7.4. The comparison of the CD spectra with the patterns of different secondary structures previously described (Figure 6.2) shows curve characteristic for the random coil for all of the peptides. Molar Circular Dichroism values are positive at n -> π* (λ≈220) and negative at π -> π* (λ≈190) for all peptides and measured at both 0.1 cm and 1.0 cm path lengths. (Figure 6.2).

References

[1] A. Shekaran and A. J. Garcia, "Extracellular matrix-mimetic adhesive biomaterials for bone repair," *Journal of Biomedical Materials Research Part A*, vol. 96A, pp. 261-272, Jan 2011.

[2] A. K. Tsao, *et al.*, "What patient and surgical factors contribute to implant wear and osteolysis in total joint arthroplasty?," *Journal of the American Academy of Orthopaedic Surgeons*, vol. 16, pp. S7-S13, 2008.

[3] N. J. Registry, "Prostheses used in hip, knee and ankle replacement procedures 2011," 9, 2012.

[4] D. A. Puleo and A. Nanci, "Understanding and controlling the bone-implant interface," *Biomaterials*, vol. 20, pp. 2311-2321, Dec 1999.

[5] C. D. Reyes, *et al.*, "Biomolecular surface coating to enhance orthopaedic tissue healing and integration," *Biomaterials*, vol. 28, pp. 3228-3235, Jul 2007.

[6] T. Hayashi, *et al.*, "Mechanism underlying specificity of proteins targeting inorganic materials," *Nano Letters*, vol. 6, pp. 515-519, Mar 2006.

[7] K. Kokubun, *et al.*, "Motif-Programmed Artificial Extracellular Matrix," *Biomacromolecules*, vol. 9, pp. 3098-3105, Nov 2008.

[8] K. I. Sano and K. Shiba, "A hexapeptide motif that electrostatically binds to the surface of titanium," *Journal of the American Chemical Society*, vol. 125, pp. 14234-14235, Nov 2003.

[9] A. D. Roddick-Lanzilotta, *et al.*, "An in situ infrared spectroscopic study of the adsorption of lysine to TiO2 from an aqueous solution," *Langmuir*, vol. 14, pp. 6479-6484, Oct 1998.

[10] A. D. Roddick-Lanzilotta and A. J. McQuillan, "An in situ infrared spectroscopic study of glutamic acid and of aspartic acid adsorbed on TiO2: Implications for the biocompatibility of titanium," *Journal of Colloid and Interface Science*, vol. 227, pp. 48-54, Jul 2000.

[11] Y. Yang, *et al.*, "How Does Bone Sialoprotein Promote the Nucleation of Hydroxyapatite? A Molecular Dynamics Study Using Model Peptides of Different Conformations," *Langmuir*, vol. 26, pp. 9848-9859, 2010.

[12] T. Hayashi, *et al.*, "Critical Amino Acid Residues for the Specific Binding of the Ti-Recognizing Recombinant Ferritin with Oxide Surfaces of Titanium and Silicon," *Langmuir*, vol. 25, pp. 10901-10906, Sep 2009.

[13] S. Roessler, *et al.*, "Biomimetic coatings functionalized with adhesion peptides for dental implants," *Journal of Materials Science-Materials in Medicine*, vol. 12, pp. 871-877, 2001.

[14] J. H. Collier and T. Segura, "Evolving the use of peptides as components of biomaterials," *Biomaterials*, vol. 32, pp. 4198-4204, Jun 2011.

[15] K. Shiba, "Exploitation of peptide motif sequences and their use in nanobiotechnology," *Current Opinion in Biotechnology,* vol. 21, pp. 412-425, Aug 2010.
[16] C. Vreuls, *et al.*, "Genetically engineered polypeptides as a new tool for inorganic nano-particles separation in water based media," *Journal of Materials Chemistry,* vol. 21, pp. 13841-13846, 2011.
[17] U. O. S. Seker and H. V. Demir, "Material Binding Peptides for Nanotechnology," *Molecules,* vol. 16, pp. 1426-1451, Feb 2011.
[18] K. Kashiwagi, *et al.*, "Directional BMP-2 for functionalization of titanium surfaces," *Biomaterials,* vol. 30, pp. 1166-1175, Feb 2009.
[19] W. Wang, *et al.*, "Orthopaedic Implant Technology: Biomaterials from Past to Future," *Annals Academy of Medicine Singapore,* vol. 40, pp. 237-244, May 2011.
[20] B. D. Briggs and M. R. Knecht, "Nanotechnology Meets Biology: Peptide-based Methods for the Fabrication of Functional Materials," *Journal of Physical Chemistry Letters,* vol. 3, pp. 405-418, Feb 2012.
[21] M. Sarikaya, *et al.*, "Molecular biomimetics: nanotechnology through biology," *Nature Materials,* vol. 2, pp. 577-585, Sep 2003.
[22] G. M. Luz and J. F. Mano, "Mineralized structures in nature: Examples and inspirations for the design of new composite materials and biomaterials," *Composites Science and Technology,* vol. 70, pp. 1777-1788, Nov 2010.
[23] M. B. Dickerson, *et al.*, "Protein- and Peptide-Directed Syntheses of Inorganic Materials," *Chemical Reviews,* vol. 108, pp. 4935-4978, Nov 2008.
[24] C. L. Chen and N. L. Rosi, "Peptide-Based Methods for the Preparation of Nanostructured Inorganic Materials," *Angewandte Chemie-International Edition,* vol. 49, pp. 1924-1942, 2010.
[25] K. I. Sano, *et al.*, "Specificity and biomineralization activities of Ti-binding peptide-1 (TBP-1)," *Langmuir,* vol. 21, pp. 3090-3095, Mar 2005.
[26] K. Sano, *et al.*, "Utilization of the pleiotropy of a peptidic aptamer to fabricate heterogeneous nanodot-containing multilayer nanostructures," *Journal of the American Chemical Society,* vol. 128, pp. 1717-1722, Feb 2006.
[27] E. D. Spoerke, *et al.*, "Enzyme Directed Templating of Artificial Bone Mineral," *Advanced Materials,* vol. 21, pp. 425-+, Jan 2009.
[28] C. Tamerler and M. Sarikaya, "Molecular biomimetics: nanotechnology and bionanotechnology using genetically engineered peptides," *Philosophical Transactions of the Royal Society a-Mathematical Physical and Engineering Sciences,* vol. 367, pp. 1705-1726, May 2009.
[29] C. Tamerler, *et al.*, "Molecular Biomimetics: GEPI-Based Biological Routes to Technology," *Biopolymers,* vol. 94, pp. 78-94, Jan 2010.
[30] H. B. Chen, *et al.*, "QCM-D analysis of binding mechanism of phage particles displaying a constrained heptapeptide with specific affinity to SiO2 and TiO2," *Analytical Chemistry,* vol. 78, pp. 4872-4879, Jul 2006.
[31] D. Khatayevich, *et al.*, "Biofunctionalization of materials for implants using engineered peptides," *Acta Biomaterialia,* vol. 6, pp. 4634-4641, Dec 2010.
[32] K. Sano, *et al.*, "Endowing a ferritin-like cage protein with high affinity and selectivity for certain inorganic materials," *Small,* vol. 1, pp. 826-832, Aug 2005.
[33] D. Wang, *et al.*, "A chimeric peptide that binds to titanium and mediates MC3T3-E1 cell adhesion," *Biotechnology Letters,* vol. 33, pp. 191-197, Jan 2011.

[34] W. J. Chung, *et al.*, "Evolutionary Screening of Collagen-like Peptides That Nucleate Hydroxyapatite Crystals," *Langmuir*, vol. 27, pp. 7620-7628, Jun 2011.
[35] J. Y. Lee, *et al.*, "Assembly of collagen-binding peptide with collagen as a bioactive scaffold for osteogenesis in vitro and in vivo," *Biomaterials*, vol. 28, pp. 4257-4267, Oct 2007.
[36] M. Gilbert, *et al.*, "Chimeric peptides of statherin and osteopontin that bind hydroxyapatite and mediate cell adhesion," *Journal of Biological Chemistry*, vol. 275, pp. 16213-16218, May 2000.
[37] J. D. Hartgerink, *et al.*, "Peptide-amphiphile nanofibers: A versatile scaffold for the preparation of self-assembling materials," *Proceedings of the National Academy of Sciences of the United States of America*, vol. 99, pp. 5133-5138, Apr 2002.
[38] E. Beniash, *et al.*, "Self-assembling peptide amphiphile nanofiber matrices for cell entrapment," *Acta Biomaterialia*, vol. 1, pp. 387-397, Jul 2005.
[39] J. Huang, *et al.*, "The effect of genetically engineered spider silk-dentin matrix protein 1 chimeric protein on hydroxyapatite nucleation," *Biomaterials*, vol. 28, pp. 2358-2367, May 2007.
[40] D. Itoh, *et al.*, "Enhancement of osteogenesis on hydroxyapatite surface coated with synthetic peptide (EEEEEEEPRGDT) in vitro," *Journal of Biomedical Materials Research*, vol. 62, pp. 292-298, Nov 2002.
[41] N. Sahai, "Modeling apatite nucleation in the human body and in the geochemical environment," *American Journal of Science*, vol. 305, pp. 661-672, 2005.
[42] A. A. Sawyer, *et al.*, "The effect of the addition of a polyglutamate motif to RGD on peptide tethering to hydroxyapatite and the promotion of mesenchymal stem cell adhesion," *Biomaterials*, vol. 26, pp. 7046-7056, 2005.
[43] E. D. Wang, *et al.*, "Elastin-Like Polypeptide Based Hydroxyapatite Bionanocomposites," *Biomacromolecules*, vol. 12, pp. 672-680, Mar 2011.
[44] E. Bouyer, *et al.*, "Morphological study of hydroxyapatite nanocrystal suspension," *Journal of Materials Science-Materials in Medicine*, vol. 11, pp. 523-531, Aug 2000.
[45] M. Amblard, *et al.*, "Methods and Protocols of modern solid phase peptide synthesis," *Molecular Biotechnology*, vol. 33, pp. 239-254, Jul 2006.
[46] E. Valeur and M. Bradley, "Amide bond formation: beyond the myth of coupling reagents," *Chemical Society Reviews*, vol. 38, pp. 606-631, 2009.
[47] W. G. Billotte, "Ceramic Biomaterials," in *The Biomedical Engineering Handbook, Second Edition*. vol. 1, J. D. Bronzino, Ed., 2 ed Boca Raton: CRC Press LLC, 2000, pp. 38-01 - 38-33.
[48] X. Y. Liu, *et al.*, "Surface modification of titanium, titanium alloys, and related materials for biomedical applications," *Materials Science & Engineering R-Reports*, vol. 47, pp. 49-121, Dec 2004.
[49] T. R. Dargaville, *et al.*, "Sensors and imaging for wound healing: A review," *Biosensors & Bioelectronics*, vol. 41, pp. 30-42, Mar 2013.
[50] J. Benesch, *et al.*, "Proteins and Their Peptide Motifs in Acellular Apatite Mineralization of Scaffolds for Tissue Engineering," *Tissue Engineering Part B-Reviews*, vol. 14, pp. 433-445, Dec 2008.
[51] D. E. MacDonald, *et al.*, "Surface analysis of human plasma fibronectin adsorbed to commercially pure titanium materials," *Journal of Biomedical Materials Research*, vol. 41, pp. 120-130, Jul 1998.

[52] D. D. Deligianni, *et al.*, "Effect of surface roughness of the titanium alloy Ti–6Al–4V on human bone marrow cell response and on protein adsorption," *Biomaterials,* vol. 22, pp. 1241-1251, 2001.
[53] R. Rousseau, *et al.*, "Temperature-dependent conformational transitions and hydrogen-bond dynamics of the elastin-like octapeptide GVG(VPGVG): A molecular-dynamics study," *Biophysical Journal,* vol. 86, pp. 1393-1407, Mar 2004.
[54] J. Y. Shen, *et al.*, "Conformation-specific Self-assembly of Thermo-responsive Poly(ethylene glycol)-b-polypeptide Diblock Copolymer," *Langmuir,* vol. 29, pp. 6271-6278, May 2013.
[55] R. A. Perez, *et al.*, "Naturally and synthetic smart composite biomaterials for tissue regeneration," *Advanced Drug Delivery Reviews,* vol. 65, pp. 471-496, Apr 2013.
[56] N. Higashi, *et al.*, "Site-specific adsorption of gold nanoparticles coated with thermo-responsive peptides," *Polymer Journal,* vol. 45, pp. 523-528, May 2013.
[57] K. Matsunaga, "Theoretical Defect Energetics in Calcium Phosphate Bioceramics," *Journal of the American Ceramic Society,* vol. 93, pp. 1-14, Jan 2010.
[58] A. Aykut-Yetkiner, *et al.*, "Effect of Acidic Solution Viscosity on Enamel Erosion," *Journal of Dental Research,* vol. 92, pp. 289-294, Mar 2013.
[59] F. Variola, *et al.*, "Nanoscale surface modifications of medically relevant metals: state-of-the art and perspectives," *Nanoscale,* vol. 3, pp. 335-353, 2011.
[60] B. K. Culpepper, *et al.*, "Tunable delivery of bioactive peptides from hydroxyapatite biomaterials and allograft bone using variable-length polyglutamate domains," *Journal of Biomedical Materials Research Part A,* pp. n/a-n/a, 2013.
[61] B. K. Culpepper, *et al.*, "Polyglutamate directed coupling of bioactive peptides for the delivery of osteoinductive signals on allograft bone," *Biomaterials,* vol. 34, pp. 1506-1513, Feb 2013.
[62] R. Fujisawa, *et al.*, "Attachment of osteoblastic cells to hydroxyapatite crystals by a synthetic peptide (Glu(7)-Pro-Arg-Gly-Asp-Thr) containing two functional sequences of bone sialoprotein," *Matrix Biology,* vol. 16, pp. 21-28, Apr 1997.
[63] M. B. Murphy, *et al.*, "Synthesis and in vitro hydroxyapatite binding of peptides conjugated to calcium-binding moieties," *Biomacromolecules,* vol. 8, pp. 2237-2243, Jul 2007.
[64] J. Schneider and L. C. Ciacchi, "Specific Material Recognition by Small Peptides Mediated by the Interfacial Solvent Structure," *Journal of the American Chemical Society,* vol. 134, pp. 2407-2413, Feb 2012.
[65] C. Treves, *et al.*, "In vitro biocompatibility evaluation of surface-modified titanium alloys," *Journal of Biomedical Materials Research Part A,* vol. 92A, pp. 1623-1634, Mar 2010.
[66] R. Fujisawa and M. Tamura, "Acidic bone matrix proteins and their roles in calcification," *Frontiers in Bioscience-Landmark,* vol. 17, pp. 1891-1903, Jan 2012.
[67] C. J. Newcomb, *et al.*, "The Role of Nanoscale Architecture in Supramolecular Templating of Biomimetic Hydroxyapatite Mineralization," *Small,* vol. 8, pp. 2195-2202, Jul 2012.
[68] M. Jullian, *et al.*, "N-terminus FITC labeling of peptides on solid support: the truth behind the spacer," *Tetrahedron Letters,* vol. 50, pp. 260-263, Jan 21 2009.

[69] B. Ranjbar and P. Gill, "Circular Dichroism Techniques: Biomolecular and Nanostructural Analyses- A Review," *Chemical Biology & Drug Design,* vol. 74, pp. 101-120, Aug 2009.
[70] R. W. Woody, "A Significant Role for High-Energy Transitions in the Ultraviolet Circular Dichroism Spectra of Polypeptides and Proteins," *Chirality,* vol. 22, pp. E22-E29, 2010.